The Classical Neural Global Workspace Baars-Franklin-McFadden's Emergent Neuromodular Consciousness: A Computational Neuromodeling Approach to Brain Systemic Central Cortical Neural Networks

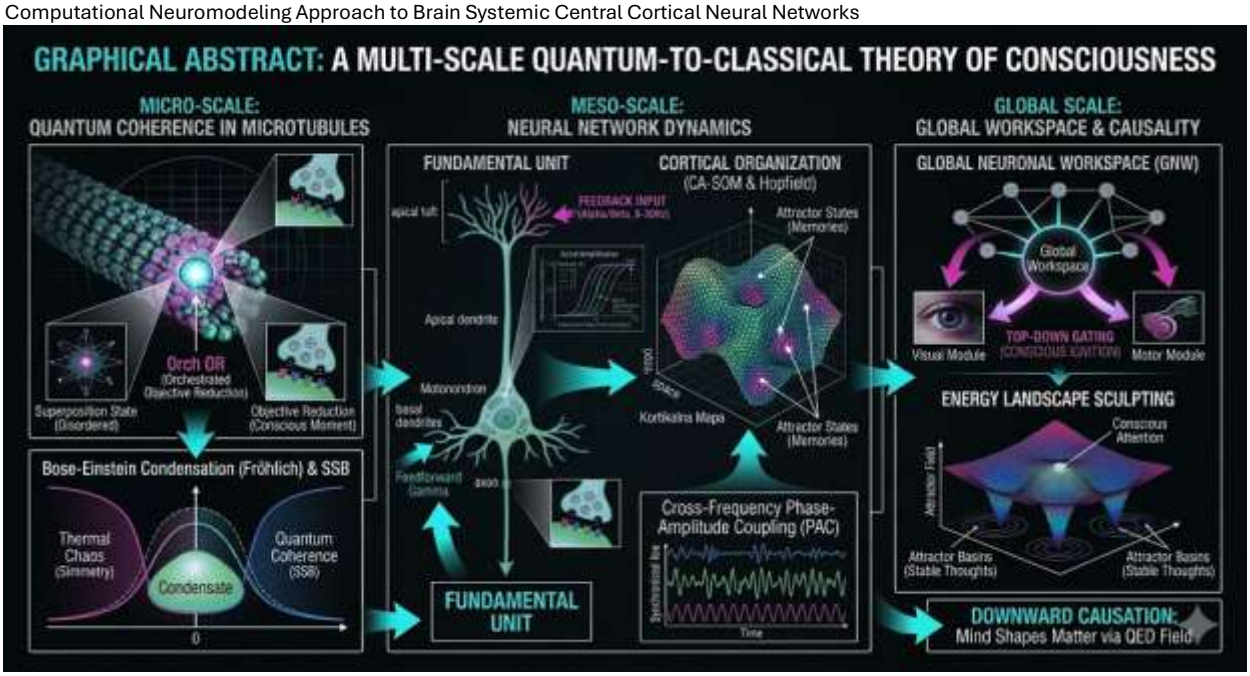
[1]Ivan Grbatinić, [2]Dejan Raković

[1]SM Medical Center, Sremska Mitrovica, Serbia
[2]Faculty of Electrical Engineering, Department of Microelectronics and Engineering Physics, University of Belgrade, Serbia

Abstract

Background: A central challenge in neuroscience is explaining how the brain's multi-scale neurostructural and neurofunctional organization gives rise to unified conscious experience. This paper proposes a comprehensive, multi-scale framework that bridges quantum brain neurodynamics with macro-scale neurobiologically grounded cognitive neuroarchitectures.
Methods: We integrate Cortical Laminar Neurocircuitry and Neuroapical Amplification computational neuromodels with Cortical Attractor Self-Organizing Maps (*CA-SOM*) and Hopfield attractor neurodynamics. This meso-scale neuroarchitecture is combined with the Kuramoto oscillatory neuromodel and paired with the physical foundations of Neuroquantum Spontaneous Symmetry Breaking (*SSB*) and the Hameroff-Penrose Orchestrated Objective Reduction (*Orch-OR*) framework.
Results: We demonstrate that conscious ignition emerges as a non-linear phase transition when neurofeedback loops (α/β frequencies) via neuroapical dendrites amplify feedforward sensory streams (γ frequencies), crossing a critical eigenvalue threshold. This laminar gain control structures the neural state space into distinct energy landscapes with stable attractor basins, optimizing dimensionality reduction. Crucially, we formalize the neural mechanism of Downward Causation of Consciousness onto Brain Systemic Neural Networks, wherein the macro-scale Global Neuronal Workspace acts as a coherent, dissipating quantum field. Through phase-locking and cross-frequency neurocoupling, this global conscious state in a retrograde manner channels energy downward, forcing quantum decoherence and micro-structural configuration within neuronal microtubule lattices.
Conclusions: Our model provides a robust theoretical and neurobiophysical bridge showing that consciousness is neither an epiphenomenon nor a purely classical computation. Instead, it operates as an active, top-down causal force that dynamically sculpts the brain's physical substrate, shifting the paradigm toward a unified neuroquantum-to-classical systems theory of mind.

Key Words: Classical Neural Consciousness, Classical Limit of Consciousness, Downward Causation



Introduction

Consciousness, in its integrated unity, specificity and subjectivity, must ultimately be explained by brain networks' neurodynamics and its underlying neurostructural and neurofunctional organizational substrate. Explaining how biological brain neural tissue gives rise to conscious experience requires a theory that is simultaneously anatomically grounded, neurophysiologically precise, dynamically formalized, and compatible with the physical constraints of matter. Contemporary computational neuroscience offers several complementary principles that map convincingly onto cortical neural circuitry: (i) (neo)cortical attractor neurodynamics in central neural recurrent networks to support stability and associative memory recall; (ii) neurotopographic self-organization to structure sensory feature spaces; (iii) recurrent and cortical laminar neural connectivity to integrate feedforward evidence with neurofeedback predictions; and (iv) large-scale neurooscillations for neurobinding and interneural communication. Contemporary cognitive computational neuroscience offers rich conceptual frameworks of consciousness such as the Global Neural Workspace Theory (*GNWT*), Integrated Information Theory (*IIT*), and recurrent processing views, each emphasizing distinct aspects of large-scale integration and neurorecurrence (1-7). At the same time, these theories propose constraints on the mechanisms that could instantiate unified conscious experience, emphasizing integration, neural reentrant interconnectivity and global accessibility (2, 4, 5, 8-10). This field of research still lacks a single computational account that threads together the canonical cortical microcircuit, thalamocortical loops, spectral multiplexing, neuromodulatory control, the thermodynamic and quantum-to-classical constraints that shape neural dynamics at scale (11-23). Yet a single quantitative neurocomputational model that begins from neocortical architectonics and neurophysiology,

specifies the neurodynamical equations for cortical attractor stability and neurotopographic mapping, shows how classical conscious contents arise, and further exhibits in parallel a principled classical limit of deeper neuroquantum substrates of consciousness has remained elusive. Here we advance such a model. We propose that consciousness, operationally understood as globally available, reportable content and the concomitant state of conscious access, can be framed as an emergent macroscopic order parameter arising from a hierarchy of recurrent neural computations implemented within laminar corticothalamic complex neural architectures. In this framing, consciousness is neither reducible to any one local neural mechanism nor divorced from physical laws: it appears when distributed cortical neuroensembles ignite into a self-sustaining yet controllable recurrent regime, and it retroacts onto its generators through gain control, synchronization, and synaptic neuroplasticity that bias subsequent neural processing (1, 2, 4, 6-8, 17, 18, 22-31). Here, our objectives are to make a unified computational Cortical Attractor–Self-Organizing map (*CA-SOM*) neural model anchored in cortical cytoneuroarchitectonics with lateral neural connectivity shaping topology. Its cortical neuromicrocolumns would serve as neural map units with neocortical laminar neurorecurrent loops as its associative cores (11, 16, 19, 32-34). We actually formalize a *CA-SOM* neuroarchitecture that integrates Hopfield associative memory with Kohonen neurotopographic organization (retinotopy, tonotopy, somatotopy) (35-39), explicitly tied to and neurobiologically implemented through neocortical neural cytoarchitectonics and neurophysiology (11, 16, 19, 32-34). This proposal synthesizes and extends multiple strands of evidence. Neurocitoarchitectonically, neocortex is organized into layered microcolumns with repeating canonical microcircuits, featuring pyramidal neurons, diverse inhibitory interneurons, and characteristic laminar neuroconnectivity motifs (16, 19, 21, 34). Hierarchically organized feedforward and feedback neuroconnections implement predictive coding-like computations, with distinct spectral channels, gamma predominating feedforward drives and alpha/beta supporting feedback hypotheses, coordinated across cortical areas and through the thalamus (11, 12, 18, 22, 23, 25, 40). In the model, sensory-driven, Kohonen neurotopology-preserving *SOM* codes provide the substrate on which recurrent attractor Hopfield neurodynamics stabilize coherent cortical neural network states. We derive the *CA-SOM* composite network energy functional, convergence, information-theoretic proxies as well as explicit neurooscillatory coupling. We further show monotone descent under appropriate asynchronous updates, establish multi-timescale convergence (fast attractor stabilization conditioned on slowly learned neurotopography), and propose information-theoretic proxies for sensory neocortical informational neurointegration. Neurooscillatory synchronization is introduced as a neuromodulatory gain and timing neural mechanism consistent with cognitive cortical rhythms (6, 41-44). Neurophysiologically, the brain flexibly toggles between metastable states, with global integration and synchrony waxing when conscious access arises and waning during unconsciousness (4, 7, 15, 45). Behaviorally and phenomenologically, the conscious access exhibits nonlinear thresholds, all-or-none ignition, and robust late signatures such as *P3b* when content enters consciousness (1-4, 6, 46). In parallel, physics constrains viable central neural mechanisms responsible for consciousness generation and sustaining. Rapid

environmental quantum decoherence in the brain renders long-lived, macroscopically relevant quantum coherence extremely unlikely at body temperature, suggesting that in so-called normal, regular states of consciousness any viable quantum consciousness must reduce to classical, stochastic effective neurodynamics at the cognition relevant scales (13, 31, 47-54). In that matter, besides the classical cortical neural architecture, we derive the *CA-SOM* energy as a classical limit of a quantum field-theoretic substrate via brain neuroquantum decoherence and stochastic quantization. We outline a neuronal microtubular field with neuroquantum spontaneous symmetry breaking (*SSB*) generating Nambu–Goldstone Boson collective modes (*NGB*) and show, via a Langevin–Fokker–Planck approach, how coarse-grained order parameters yield an effective, thermodynamically interpretable energy, mapping to *CA-SOM* attractor landscapes (55-65). This quantum-to-classical derivational approach is not intended as an empirical commitment to specific subneuronal mechanisms, which still remain debated (31, 48, 66, 67) but as a disciplined theoretically-neurocomputational pathway demonstrating how a hypothetical quantum substrate of consciousness could reduce to the proposed classical neocortical neural network while preserving computational neurostructure. Finally, we formalize retrograde neurofeedback: a conscious attractor state can modulate the cortical neural maps and neuroreverberation recurrent gains that sustain it, implementing top-down influence, predictive coding, and ignition-like broadcasting (2, 9, 11, 28, 68-72). We provide explicit neurofeedback terms that (i) tilt the attractor landscape to favor consistent interpretations, (ii) gate Kohonen *SOM* neuroplasticity and neighborhood radii to refine relevant feature neural codes, and (iii) modulate oscillatory neurocoherence to enhance effective neural connectivity. We derive stability conditions for these closed neural loops and state testable neurophysiological predictions. Additionally, by finding quantum-to-classical limit via quantum decoherence and stochastic quantization that yields an effective energy of the model, we find the corresponding *CA-SOM* neurodynamics (55, 56, 58, 59, 61, 63-65) and formulate retrograde feedback laws whereby conscious attractors modulate bottom-up neural maps and recurrent gains, consistent with *GNWT* ignition and predictive neural coding (2, 9, 11, 28, 68-72). This computational neuromodel of consciousness explains why cortical neurocytoarchitectonic structure matters at the classical neural organizational level of consciousness emerging from it: the cortical columnar neurotopology and laminar neural recurrence do not merely correlate with conscious contents; they instantiate the necessary operations - dimensionality reduction with neurotopological preservation for compositional neurostructure and neural neocortical attractor stabilization for integrated, definite conscious contents. Conscious access, in the model, is the system's fast settling into a neurotopologically anchored, globally stable cortical network neuroattractor, with retrograde neurofeedback that tunes the substrate to maintain, refine, or shift conscious content. The quantum-to-classical analysis shows one way, in principle, that such classical cortical network neurodynamics could still emerge from a deeper, noisy, symmetry-breaking quantum field with long-range correlations, without violating quantum decoherence constraints at physiological temperatures, by-passing that way the warm, wet and noisy brain environment as relevant for neuroquantum consciousness (31, 65). To coordinate these threads into a predictive and testable account, we introduce a multiscale

theoretical modeling framework with three central claims. First, classical brain neural network processes, explicitly modeled via mean-field reductions from spiking neurons, spectral synchronization neurodynamics, and neurohierarchical predictive coding energy functions, are sufficient to generate a macroscopic order parameter $C(t)$ indexing conscious access. This $C(t)$ corresponds to global neural workspace ignition, measurable through distributed brain neural activity, information integration surrogates, and cross-frequency neural synchronization (1-7, 12, 22, 25, 73). Second, the $C(t)$ can be also understood on the other hand as the classical limit of any putative sub-neural quantum brain neuroprocesses: by starting from a general Lindblad master equation for open quantum systems and passing to a Fokker–Planck-Langevin description via the Wigner transform and Kramers–Moyal expansion, we obtain stochastic, nonlinear classical neurodynamics that integrate seamlessly with the mean-field neural equations. In this limit, neuroquantum reduces to noise, renormalized parameters, and effective nonlinearity, with quantum neurodecoherence times far too short to preserve macroscale coherence in warm, wet brain environment (13, 31, 47, 48, 74-77). Third, the emergent macroscopic $C(t)$ retroacts onto its own substrates through gain modulation, thalamocortical neurocoupling, and neuromodulated three-factor learning rules. This retrograde feedback stabilizes ignition, shapes neuroplasticity for credit assignment, and explains why consciousness access correlates with arousal, pupil dilation, and performance improvements (23-30, 78). Our theoretical computational neuromodeling study derives the governing equations of the model at each scale, specifies clear boundary conditions of the model and bifurcation criteria for neuronal ignition, and shows how $C(t)$ couples to spectral synchrony, neuromodulatory state, and neurosynaptic plasticity. We avoid relying on any single theory's axioms; instead, we demonstrate how the canonical cortical microcircuit and thalamocortical loops, subject to physical constraints, generate the macroscopic phenomena indexed by existing consciousness measures (e.g., late reports, the *P3b*, the perturbational complexity index) (1-4, 6, 46, 73). This approach aims to be falsifiable by making quantitative predictions about the timing and neurotopology of ignition, the dependence of cross-frequency coupling on laminar neurofeedback, and the sensitivity of retrograde gain control to neuromodulatory manipulations. We begin by formalizing the emergent order parameter $C(t)$ from cortical mean-field neurodynamics, showing how ignition results from an eigenvalue crossing that is modulated by apical amplification, cortico-thalamic neurosynchrony, and neuromodulatory gain (4, 11, 12, 18, 20, 22, 23, 79). We then demonstrate the neuroquantum-to-classical reduction, clarifying the specific ways in which putative quantum contributions enter the classical neural equations, namely, as stochastic drive and parameter renormalization, without requiring macroscale quantum coherence (13, 16, 31, 47, 48, 74-77). Finally, we formalize the retrograde neural loop, where $C(t)$ feeds back onto cortical networks through a control law that adjusts neural gains, neural synchrony, and neuroplasticity. These results, taken together, argue that consciousness is an emergent, neurodynamical property of the complex neocortico–thalamic–neuromodulatory system, a property that is quantitatively definable, physically grounded, and mechanistically constructive. The broader implications of this framework are three-fold. Theoretically, it reconciles key empirical signatures emphasized by *GNWT* and recurrent processing accounts with constraints from

predictive coding, neurodynamical systems, and statistical physics (4, 7, 11, 15, 17, 80, 81). Methodologically, it suggests protocols for perturbation-based measurement and control of $C(t)$, including closed-loop neuromodulation and laminar-specific stimulation to bias feedback channels (23, 25, 73). Clinically, it refines anesthesia biomarkers and disorders of consciousness by targeting the transitional neurodynamics at ignition thresholds, the coupling between alpha/beta feedback and gamma feedforward, and the neuromodulatory levers that regulate gain and neurosynchrony (4, 23, 24, 29, 30, 73, 78, 82). Alongside with first providing explicit derivations of the model and quantitative statements, we further evaluate the conceptual coherence of the proposed model framework, its relationship to existing theories, and its near-term empirical tests.

Methods

In this theoretical study, a multiscalar computational neuromodeling approach was applied that integrates the classical neurodynamics of neuronal populations of cortical neuroensembles with the principles of statistical mechanics and quantum field theory (*QFT*). We employ derivation of theoretical implications of the model and integration of model predictions with experimental data. The modeling was carried out through four key levels:

System Neurodynamics and Global Ignition Modeling

A mean-field formalism derived from the stochastic differential equations of Leaky Integrate-and-Fire (*LIF*) neurons was used here. Global ignition is modeled as a bifurcation (crossing of Jacobian eigenvalues) within hierarchically coupled cortical areas, where neuroapical amplification and thalamocortical neurosynchronization act as control parameters of neuroamplification.

Defining CA-SOM Neural Architecture

A hybrid neurocomputational model was formed that integrates Kohonen *SOM* for neurotopographic coding of sensory features and Hopfield associative network for stabilizing conscious content in the form of attractors (**Fig. 1**). The stability of the system is proven through the composite energy functional E_C which ensures monotonic convergence towards stable states.

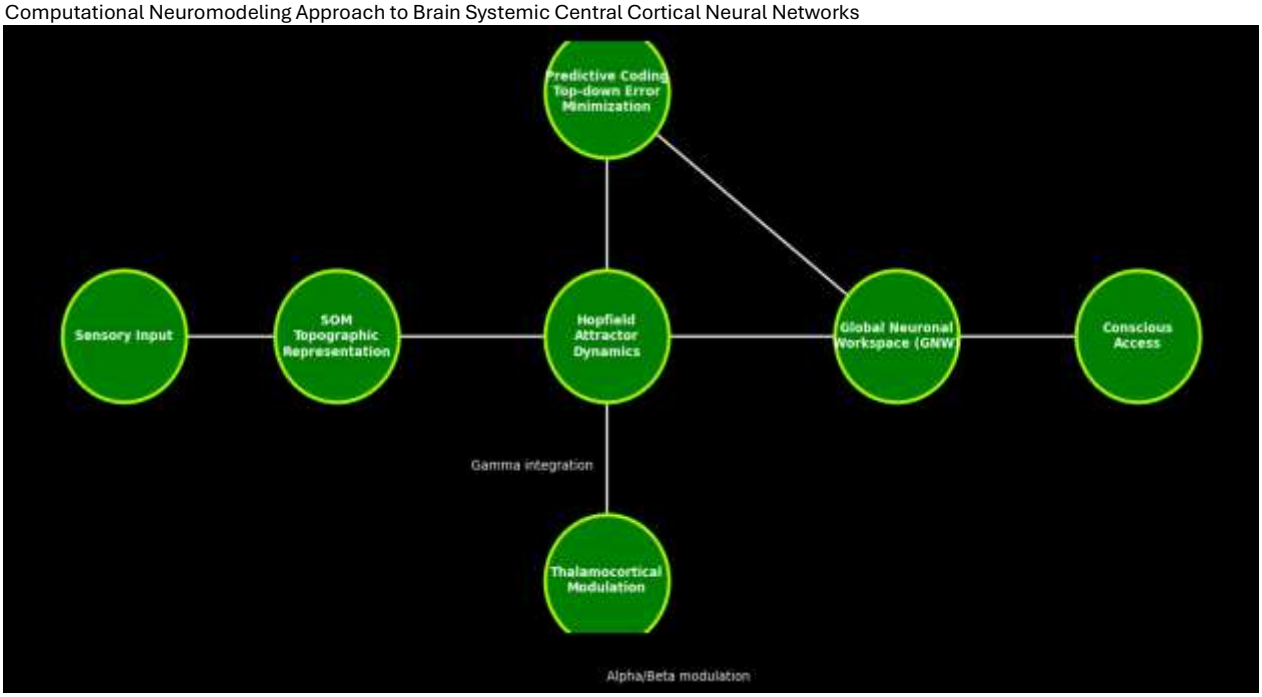


Fig. 1. Integrative Computational Neuroarchitecture of the Proposed Combined Classical Neural Model of Consciousness (*CA-SOM*). Sensory information is first organized into neurotopographic representations via Kohonen *SOM* neurodynamics, followed by cortical attractor stabilization through Hopfield mechanisms. Predictive coding, thalamocortical neuromodulation, and global neuronal workspace interactions jointly enable consciousness.

Spectral Multiplexing and Neurosynchronization Modeling

Coordination of cortically distributed Baars-Franklin's neuromodules is modeled using the Kuramoto formalism of phase oscillators. A macroscopic order parameter $C(t)$ is introduced that quantifies conscious access as a function of neurocoherence in the gamma (feedforward) and alpha/beta (neurofeedback) bands, including cross-phase-amplitude neurocoupling.

Quantum-to-Classical Reduction

The transition from microscopic neuroquantum processes (Lindblad equation) to macroscopic classical variables via stochastic quantization and the Langevin-Fokker-Planck approach was theoretically performed. By starting from a general Lindblad master equation for open quantum systems and passing to a Fokker–Planck-Langevin description via the Wigner transform and Kramers–Moyal expansion, we obtain stochastic, nonlinear classical neurodynamics that integrate with the mean-field neural equations. It is shown how the thermodynamic limit and decoherence in the warm and wet environment of the brain result in an effective energy landscape corresponding to the *CA-SOM* model. Finally, the model formalizes downward causation through control laws that modify neuronal gain and neurosynaptic plasticity based on the current state of the $C(t)$ parameter.

Neurocytoarchitectonically and Neurophysiologically based Consciousness-Generating Classical Neocortical System Neural Network Processes – Classical Neural Consciousness Emergence

From Spiking Neurons to Mean-Field Ignition: Cortical Neuroensemble Neural Network Neurodynamics

We start from a cortical *LIF* neuronal population of cortical neuroensembles with single-neuron neuromembrane potential $V_i(t)$ obeying the following differential equation (**Fig. 2**),

$$C_m \frac{d}{dt} V_i = \sigma_i \xi_i(t) - g_L(V_i - E_L) + I_{ext,i}(t) + I_{syn,i}(t),$$

where C_m is membrane capacitance, g_L is leakage conductance, E_L is reverse leakage potential, $I_{syn,i}$ defined by

$$I_{syn,i} = \sum_j W_{ij} s_j(t),$$

is synaptic input (recurrent and/or feedforward) from presynaptic spikes s_j, W_{ij} is synaptic weight (matrix) between them, $I_{ext,i}$ is external drive (stimulus) and $\sigma_i \xi_i(t)$ gives effective Gaussian white noise approximation. Such stochastic neuromembrane dynamics provides a biophysically grounded neurophysiological and neurofunctional substrate in which neuromembrane filtering and intrinsic noise give rise to smooth effective transfer functions at the population neuronal, neuroensemble level. Under standard diffusion approximations, the stochastic neuromembrane equation leads to a continuous firing-rate nonlinearity, justifying the use of smooth neuronal population transfer functions (12, 74, 75, 79). Under the diffusion approximation and assuming a stationary neural input distribution, the firing rate $r_i(t)$ of an i-th neuron can be approximated as a smooth function of its mean input μ_i and variance v_i, i.e.

$$r_i(t) \approx f[\mu_i(t), v_i(t)],$$

where $f[\cdot]$ is the transfer function derived from first-passage time analysis for *LIF* neurons (79). Aggregating, segregating and organizing neurons further into local excitatory (*E*) and inhibitory (*I*) neuroensemble pools yields

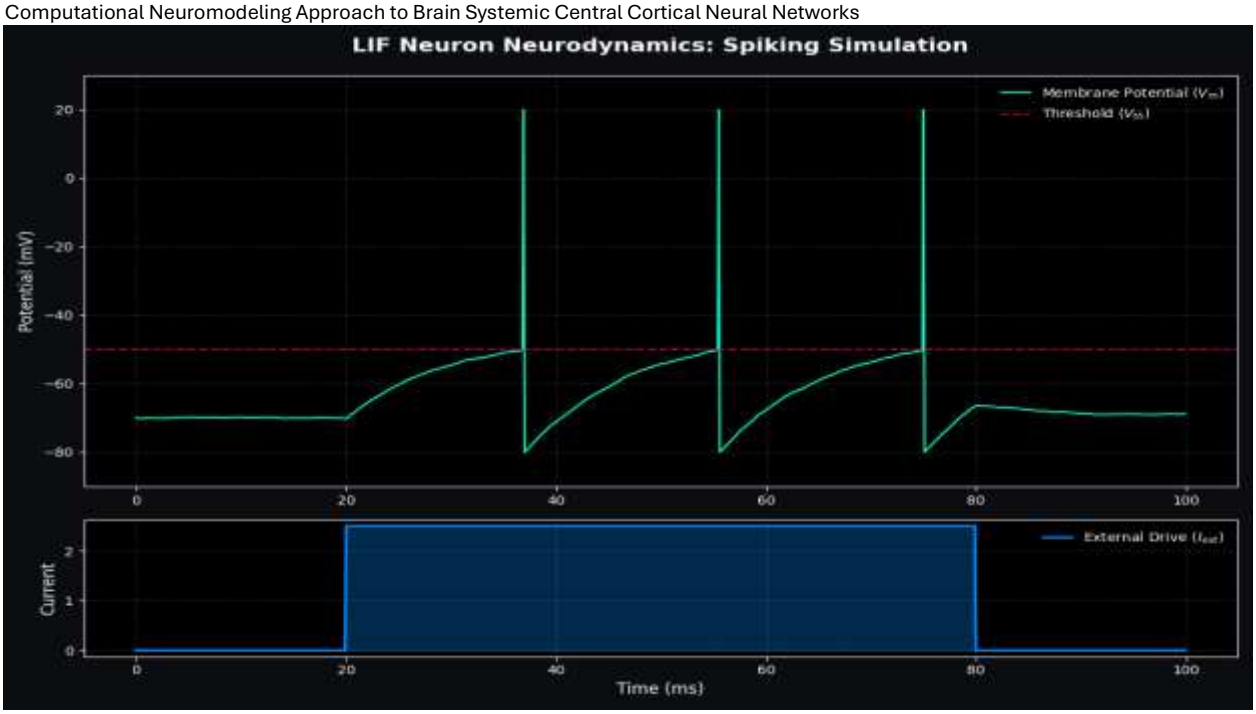


Fig. 2. Cortical *LIF* Neuron. Action potential electric-triggering firing activity of a *LIF* cortical neuron on an external stimulus neurosignal.

Wilson–Cowan mean-field neurodynamics (**Fig. 3**) given by a minimal aggregate computational neuromodel of excitatory-inhibitory neural balance and nonlinear amplification, described by the following differential system of equations,

$$\frac{d}{dt}E = F_E\big(I_E + w_{EE}E - w_{EI}I + \eta_E(t)\big) - E,$$

$$\frac{d}{dt}I = F_I\big(I_I + w_{IE}E - w_{II}I + \eta_I(t)\big) - I,$$

where E and I actually mean activities of excitatory and inhibitory neuroensembles, respectively, w defines effective synaptic coupling strengths between excitatory/inhibitory neurons, F_E and F_I are the corresponding (excitatory or inhibitory) non-linear sigmoid transfer functions derived from *LIF* analysis and $\eta_{E/I}$ is the corresponding synaptic and intrinsic noise (12, 74-77, 79). This makes the neurofunctional foundation for cortical large-scale neurodynamics. As we will demonstrate this more extensively later for the real, full, complete case, but still showing and outlining its essence, significance and principle now, the global role of it is reflected by

extending this further to for now a very simple neuromodel of neural networks of cortical areas indexed by a and b, each with laminar structure of course, with $\boldsymbol{x}_{a/b}$ denoting a vector of the corresponding neuroensemble neuroactivities (e.g., superficial/deep E/I). Coupling across the areas follows the neurostructural hierarchy (hierarchically connected areas with laminar specific channels) (11, 19, 40), generally given by

$$\frac{d\boldsymbol{x}_a}{dt} = F_a\left(\boldsymbol{I}_a + \sum_b W_{ab}\,x_b + \boldsymbol{\eta}_a(t)\right) - \boldsymbol{x}_a,$$

where $\boldsymbol{x}_a$ is the vector of laminar neuroensemble activities in area a, W_{ab} is general synaptic weight matrix structured as a neuroconnectivity tensor specific for this,

cortical neuroarchitectonics and inter-neuroconnection patterns, thus simultaneously implementing feedforward (superficial to layer 4), neurofeedback (deep to superficial/neuroapical) and lateral interneural interactions all together without specific addressing for now (11, 16, 19, 21, 40); we do this later. F_a is functional nonlinearity with

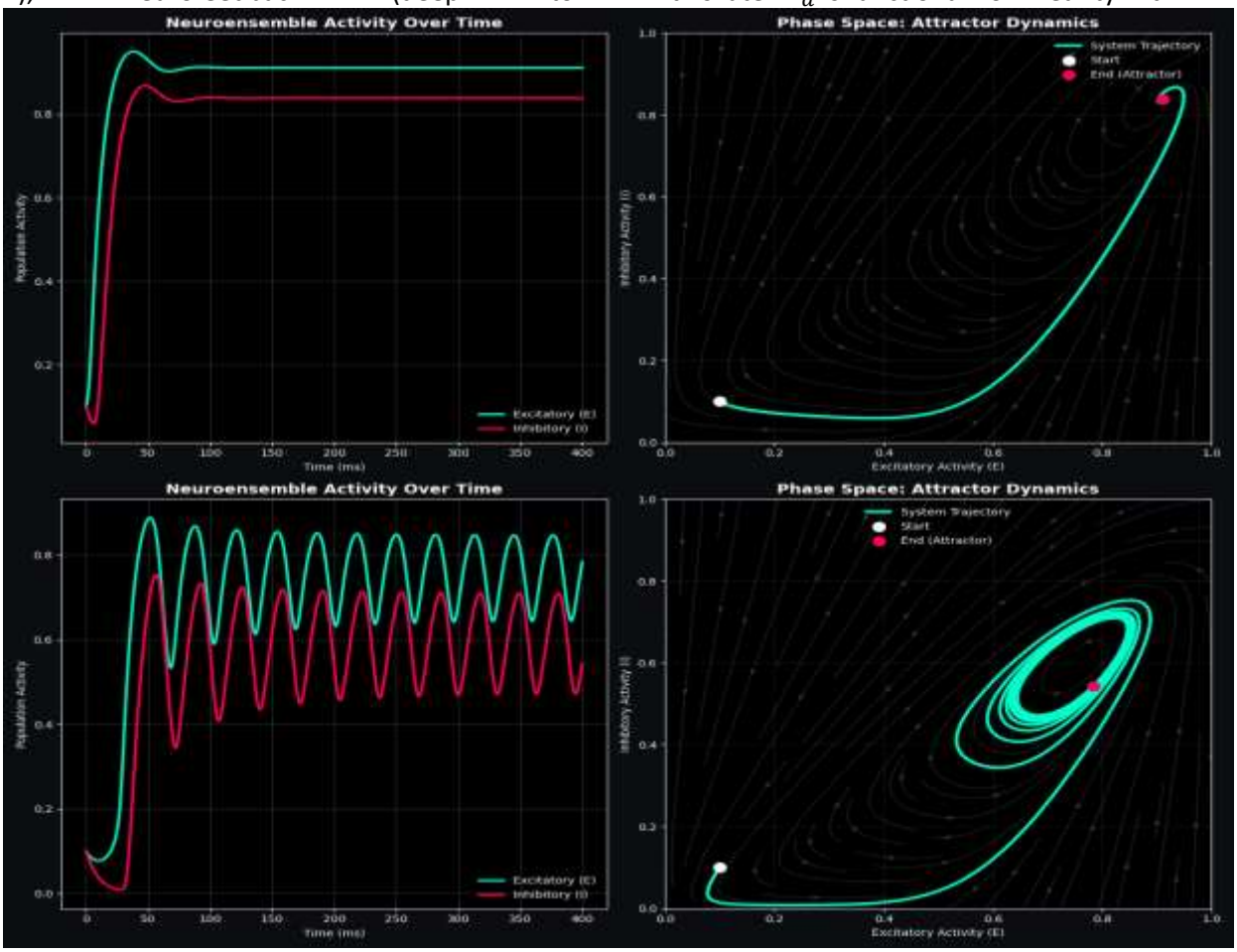


Fig. 3. The Computational Model of Wilson-Cowan Neurodynamics. Temporal neurooscillations **(Left)**: You can see how the *E* and *I* populations of neurons of cortical neuroassemblies follow each other. This is the basis for the γ and α/β neurocortical rhythms. **Phase Space Portrait (Right):** The phase space arrows show the flow of the system. The path **(cyan line)** literally falls into the stable attractor state of consciousness. **Bifurcation:** A change of external input to lower values (from 1.5 **(Top)** to 0.3 **(Down)**), turns the system from a stationary fixed point attractor (unconscious state) **(Top)** into a stable neurodynamic limit cycle of the phase space with sustained mutual γ-neurooscillatory behaviour between *E* and *I* neuroensembles (the moment of Consciousness Ignition).

possible neuroapical amplification, modeled as a multiplicative gain on basal input controlled by neuroapical depolarization $A_a(t)$ (20),

$$F_a(z; A_a) = \phi[g_0 z(1 + A_a\beta) - \theta],$$

where $\phi[\cdot]$ is sigmoid smooth nonlinearity (e.g. logistics), g_0 is base gain, β is neuroapical modulation influence quantifier coefficient, $\boldsymbol{I}_a$ is external neurosignal of a sensory stimulus, $\boldsymbol{\eta}_a$ is noise and θ is neuroactivation threshold.

Thus, deep neurofeedback information multiplicatively amplifies the basal inputs. Linearizing around a fixed, working point x^*, we

obtain the bifurcation criterion of global neuropopulation inclusion, i.e. neuronal ignition,

$$\frac{dx}{dt} = Jx + u,$$

where

$$J = WD_F(x^*) - I,$$

is the Jacobian, D_F is the diagonal Jacobian matrix of nonlinearities (derivatives of F at x^*), and u summarizes inputs and noise. *LIF* neural ignition corresponds to the largest real part of eigenvalues of J crossing zero: $max\ Re\ \lambda(J) > 0$ triggers and indicates a transition from a stable fixed point to a self-sustaining high-activity metastable regime/mode (2, 4, 46, 83) . Therefore, conditions for the global neuroensemble ignition include: (i) strong neural recurrent excitation W_{EE}, balanced by inhibition, raises the slope of F around x^*, (ii) neuroapical amplification increases D_F via $A_a(t)$ driven by neurofeedback signals, thus effectively increasing neural gain $g_0(1 + A_a\beta)$, (iii) thalamocortical synchrony increases effective W by enhancing neural phase alignment and effective neurocoupling (18, 22, 23, 25), and finally (iv) synaptic neuromodulators increase gain and reduce adaptation, shifting ϕ to steeper slopes (24, 29, 30). Together, these factors push the neural system to an eigenvalue crossing, generating the observed nonlinear threshold for conscious access (46). The bifurcation can be saddle-node or sudden, subcritical Hopf depending on delays and neurooscillatory couplings. Therefore, in either case, a *LIF* neurodynamically based, metastable neurooscillatory state is achieved which is essential for informational neurocoupling and integration necessary for consciousness. Empirically and clinically, as a mere neurofunctional correlate of the computationally modeled cortical *LIF*-based neurodynamics, we then can see late *P3b*-like bursts suggesting a rapid large-scale recruitment consistent with such found and theoretically observed neurophysiological bifurcations (2, 4, 46).

Laminar Neuroapical Amplification

While the *LIF*-based mean-field formulation captures the effective input–output transformation of neuronal population of cortical neuroensemble networks, it does not yet specify the neurobiological mechanisms that neurodynamically regulate neuronal gain. In the neocortex, such gain neuromodulation is critically mediated by dendritic neurointegration, particularly through neuroapical tuft inputs. We therefore extend the neuroensemble neuronal population description by incorporating laminar neuroapical amplification (**Fig. 4**) as a key neurobiophysical mechanism controlling effective neural responsiveness. Dendritic neurointegration in cortical pyramidal neurons provides a mechanistic basis for top-down/bottom-up interneural interactions. The neuroapical tuft in layer 1 receives neurofeedback and neuromodulatory inputs that can amplify basal compartment-driven spikes via calcium-mediated dendritic events, allowing neurofeedback to gate or amplify feedforward inputs (20). We model the postsynaptic gain g_{eff} as

$$g_{eff} = g_0(1 + \beta A),$$

with neuroapical depolarization A obeying a neurodynamic equation reflecting neurofeedback drive,

$$\tau_A \frac{dA}{dt} = h(FB) - A,$$

where FB reflects deep-layer neurofeedback inputs and $h(\cdot)$ is a saturating nonlinear function, τ_A is the time constant of neuroapical processes. This gives a neural process by which neurofeedback multiplicatively enhances

feedforward mechanism. Substituting g_{eff} into F_a above shows how neurofeedback can neurodynamically move the system across ignition thresholds by neuromodulating local gains, and explains at that level of neural classicality and causation why laminar disruption (e.g., in anesthesia) reduces consciousness access (4, 20).

Cortical Area Network and Hierarchical Neural Coupling

Having established the cortical translaminar mechanisms of local gain neuromodulation through neuroapical amplification, we are now ready to extend the framework of single-area neuroensemble neurodynamics to the real, full-model large-scale neocortical system composed of hierarchically organized cortical areas indexed by $a, b \equiv \{1, \dots, N_a\}$. Cortical informational neuroprocessing is not confined to isolated neural microcircuits but emerges from the interaction of distributed, hierarchically organized cortical areas. These areas are neurally coupled through structured feedforward and neurofeedback projections

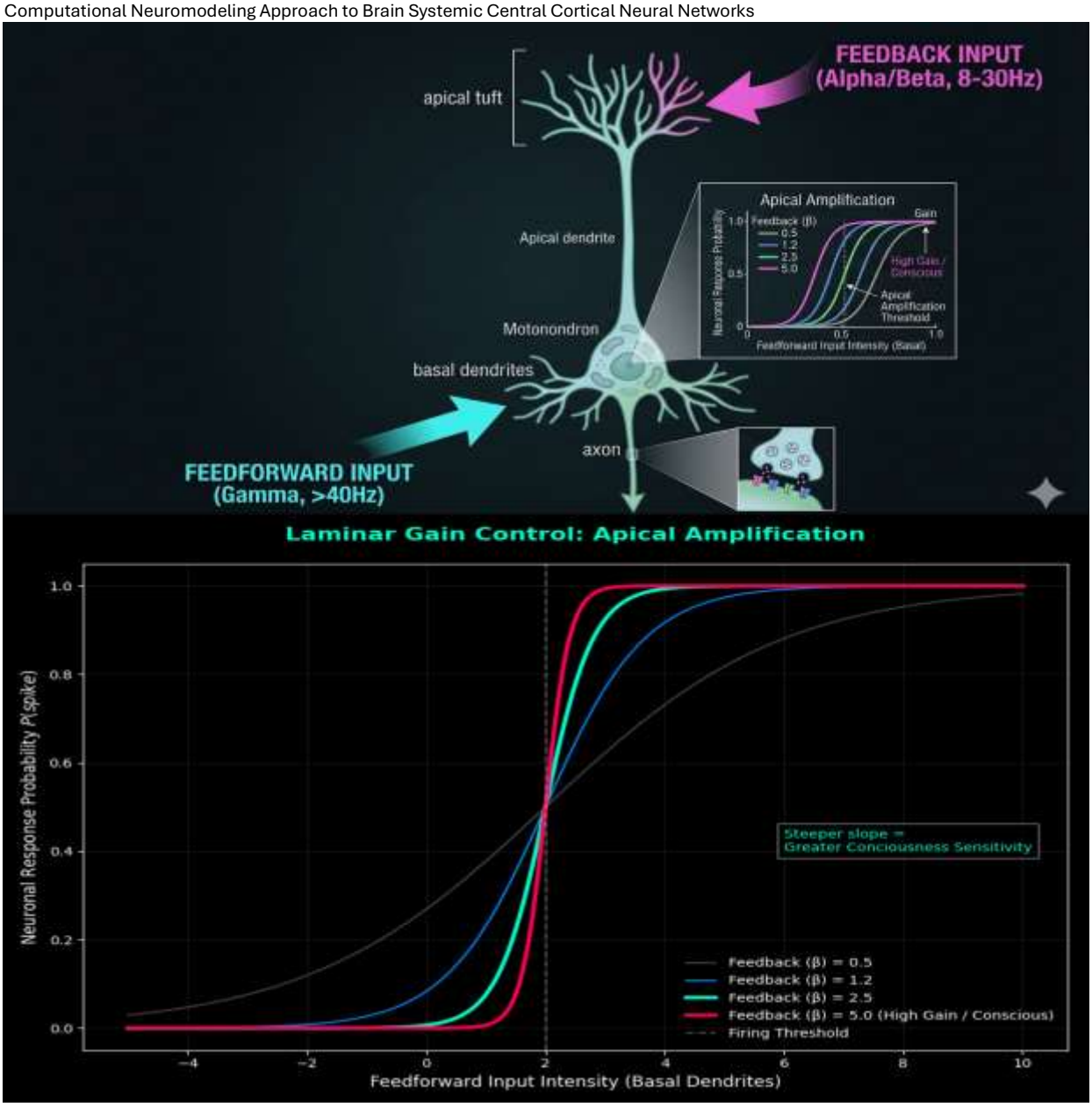


Fig. 4. Consciousness-Dependent and Consciousness-Generating Neuromodulatory Multiplicative Gain and Neuroapical Amplification. (Top) Neurohistological schematics of neurofunctional neuroapical amplification process. **Nonlinear Gain (Down):** We can see how the gray line ($\beta = 0.5$) barely reacts, while the pink line ($\beta = 5.0$) reacts lightning fast. Consciousness amplifies important information and ignores unimportant one. **Cortical Translaminar Neurofeedback:** This computational neuromodel explains why in an unconscious state (e.g. anesthesia, where neurofeedback is blocked) the brain still receives neurosignals, but the neurons do not fire strongly enough for the information to become global.

that respect laminar specificity and preserve directional information flow. The resulting

neuroarchitecture defines a multi-area distributed neurodynamical system in which local neuroensemble neurodynamics are

embedded within a global neural hierarchical network, enabling context-dependent integration across spatially distributed cortical Baars-Franklin *GWNS* neuromodules. Each cortical area is itself a structured laminar neuroensemble, such that its state is represented now by the real, abovementioned cortical vector of laminar neuroactivities given by

$$\boldsymbol{x}_a(t) = \left(x_a^{(sup)}(t), x_a^{(deep)}(t), x_a^{(in4)}(t)\right),$$

corresponding to superficial, deep, and granular (layer 4) neuronal populations. The interareal neurodynamics is governed by structured hierarchical neurocoupling, reflecting transareal feedforward and feedback projections constrained by cortical laminar neuroarchitecture. The full network neurodynamics can be written as

$$\tau \frac{d\boldsymbol{x}_a}{dt} = \phi\left(\boldsymbol{W}^{(local)}\boldsymbol{x}_a + \sum_b W_{ab}^{(FF)}\, x_b^{(sup)} + \sum_b W_{ba}^{(FB)}\, x_b^{(deep)} + \boldsymbol{I}_a(t) + \boldsymbol{\xi}_a(t)\right) - \boldsymbol{x}_a,$$

where $\boldsymbol{W}^{(local)}$ encodes intra-areal recurrent laminar neuroconnectivity, $W_{ab}^{(FF)}$ implements feedforward projections (superficial → granular input layers), $W_{ab}^{(FB)}$ implements neurofeedback projections (deep → superficial neuromodulation), $\phi(\cdot)$ is a nonlinear transfer function inherited from *LIF* diffusion reduction, $\boldsymbol{I}_a$ is external thalamocortical or sensory drive and $\boldsymbol{\xi}_a$ is effective mesoscale noise. Importantly, the interareal neurocoupling tensors obey a hierarchical constraint consistent with neocortical structure:
$\boldsymbol{W}_{ab}^{(FF)} \gg \boldsymbol{W}_{ab}^{(FB)}$, for lower-to-higher transitions,
$\boldsymbol{W}_{ab}^{(FB)} \gg \boldsymbol{W}_{ab}^{(FF)}$, for higher-to-lower transitions, ensuring directional asymmetry of information flow across the cortical hierarchy. To incorporate laminar specificity, we define structured cortical routing functions,
$\mathcal{R}_{FF}: \boldsymbol{x}_b^{(sup)} \to \boldsymbol{x}_a^{(in4)}$, $\mathcal{R}_{FB}: \boldsymbol{x}_b^{(deep)} \to \boldsymbol{x}_a^{(sup)}$
which implement feedforward driving of sensory evidence and neurofeedback predictive neuromodulation, respectively. The resulting neural system actually now defines a hierarchically nested recurrent neurodynamical system, in which each cortical area functions as a locally stable but globally neurally coupled nonlinear node. This neuroarchitecture enables both local attractor formation and global neurocoordination across distributed cortical regions. The stability of the full system is determined by the spectrum of the block Jacobian:

$$\mathcal{J} \equiv \begin{bmatrix} J_{11} & J_{12} & \cdots & J_{1N} \\ J_{21} & J_{22} & & J_{2N} \\ \vdots & & \ddots & \vdots \\ J_{N1} & J_{N2} & \cdots & J_{NN} \end{bmatrix},$$

where each block J_{ab} encodes intra- and interareal gain-modulated neurocoupling. Conscious-state transitions actually correspond to global eigenvalue crossings of this block operator, thus extending the single-area ignition mechanism to a global distributed cortical regime as its detectable and measurable classical neural neurophysiological correlate. We explain this further.

Consciousness Ignition as an Eigenvalue Crossing and Hysteresis

Within such hierarchically coupled cortical networks, local nonlinear amplification and neurorecurrent interactions give rise to global neurodynamical transitions. In particular, the interplay between neural excitation, inhibition,

and neurofeedback-driven gain neuromodulation enables the emergence of large-scale instabilities. These instabilities manifest as bifurcations in the system neurodynamics, thus resulting and corresponding to the phenomenon of neuronal ignition. Let $J(C)$ be the Jacobian when control parameters (gains and neurocouplings) depend on C via neurofeedback. A saddle-node bifurcation occurs when the largest eigenvalue crosses zero at parameter value p_c. For a scalar gain g, the stability change condition is $det\big(J(g_c)\big) = 0$ (formal criterion of ignition - zero eigenvalue) with

$$\frac{d}{dt}\, max\, Re\, \lambda(J) > 0, \text{at } g = g_c,$$

where g is a scalar gain parameter, g_c is a critical transition value. The presence of positive neurofeedback creates hysteresis: the up-threshold g_{up} for ignition is higher than the down-threshold g_{down} for de-ignition, consistent with the persistence of conscious content under brief masking differences (46). Additionally, the obtained consciousness-stabilizing balanced neuroamplification across areas further stabilizes obtained transcortical neurosignal propagation thus enabling positive feedback self-sustaining neural process (83).

Spectral Multiplexing, Thalamic Coordination and Order Parameter

While neural ignition describes the transition to a high-activity metastable regime, conscious processing additionally requires another essential phenomenon, and that is neurocoordination across distributed cortical neuroensembles. This neural coordination is actually achieved through neurofunctionally implemented phase synchronization of neural oscillations, so-called spectral multiplexing (**Fig. 5**), predominantly realized at the level of the great thalamocortical neuroreverberation. We therefore complement the rate-based description with a phase-based formalism, modeling large-scale neural coherence using coupled oscillator neurodynamics. Cortical feedforward neurosignaling is preferentially carried by gamma-band neural synchronization, whereas neurofeedback rides alpha/beta rhythms, a pattern observed across primate visual cortex and inferred across the neurohierarchy (12, 22, 25). We model phase neurodynamics of local neurooscillators with intrinsic frequencies ω_i and additive noise using Kuramoto phase neurodynamics (**Figs. 6, 7**) (84),

$$\frac{d\theta_i}{dt} = \omega_i + \frac{K}{N}\sum_j a_{ij} sin\big(\theta_j - \theta_i\big) + \zeta_i(t),$$

with adjacency (neurostructural-functional mask) a_{ij} reflecting neurostructural and neurofunctional couplings (including thalamic relay), θ_i is local neurooscillator phase, K is a global neurocoupling coefficient, $\zeta_i(t)$ is phase noise. Thus, critical pairing (K_c) drives macroscopic neurosynchronization. The global neural synchrony is quantified by the order parameter, a compact measure of neurocommunication through neurocoherence,

$$Re^{i\Psi} = \frac{1}{N}\sum_j e^{i\theta_j},$$

where $0 \le R \le 1$ is a synchrony module with extremes 0 – non-synchronous and 1 – perfect synchrony, Ψ is average phase of the set of neurooscillators. In the mean-field limit, a critical neurocoupling K_c sets the onset of neurosynchrony (84). We partition neurooscillators into bands and layers: gamma neurooscillators in superficial layers (feedforward) and alpha/beta in deep layers (neurofeedback). Thalamic nuclei, especially pulvinar, provide dynamic neurocoupling that coordinates interareal neurocoherence and resolves cortical routing under conscious attention and focus (18, 23). We define band-specific order parameters R_γ and $R_{\alpha\beta}$ (neural synchrony by feedforward/feedback channels)

and model cross-frequency interactions via phase-amplitude coupling (12, 14, 25, 85):

$$A_\gamma(t) = A_0 + \kappa\cos\big(\theta_{\alpha\beta}(t) - \phi\big),$$

where A_γ is amplitude of gamma oscillations, $\theta_{\alpha\beta}$ is phase of slower (alpha/beta) rhythms, κ is strength of cross-frequency neuromodulation and ϕ is phase shift. This indicates that gamma amplitude is modulated by alpha/beta phase. Top-down (alpha/beta) rhythms neuromodulate feedforward (gamma) channels. Empirically, such cross-frequency coupling correlates with effective interneural communication and top-down control (14, 25). The thalamus increases effective K and aligns phases across nodes; task demands increased K selectively for relevant subnetworks (18, 23). We propose a macroscopic order parameter $C(t)$ capturing conscious access as a composite of neuroactivation and neurosynchrony,

$$C(t) = R_{\alpha\beta}(t)R_\gamma(t)\sigma[\alpha^T x(t) - \theta_c],$$

where σ is a logistic squashing function, α-vector weights high-order association frontoparietal areas, and θ_c sets the activation

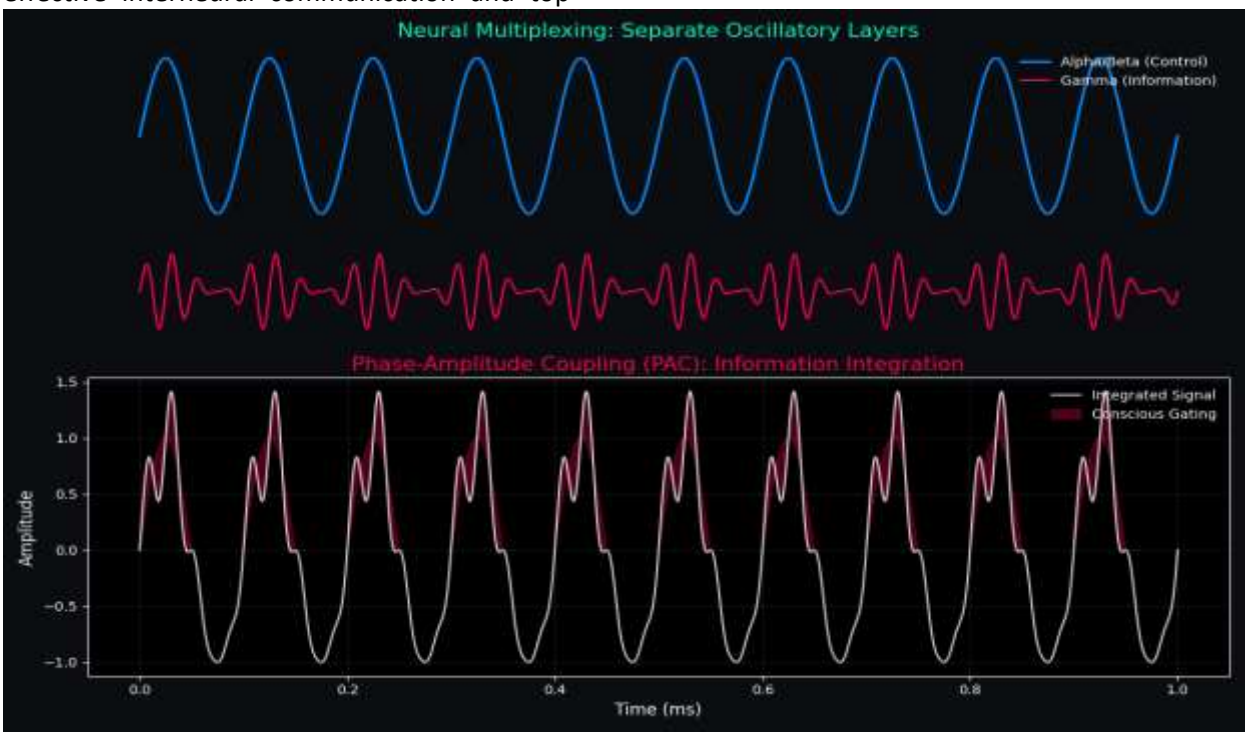


Fig. 5. Thalamocortical Multiplexing. Neural Gating: We can see how the cortical γ-rhythm does not dominates all the time **(Middle/Red)**, but the slow wave **(Top/Blue)** releases it only at certain moments. **Selective Information Neurointegration (Down):** Slow **(Top/Blue)** and Fast **(Middle/Red)** signals merge into one functional whole, i.e. neurocoherence that defines a level of consciousness. **Coordination of Neuroactivity:** Without neural synchronization, information would be chaotic. Phase-Amplitude Neurocoupling (*PAC*) is the way in which Kuramoto neurodynamics achieves order.

threshold. The product requires both activation and neurosynchrony across feedforward and feedback channels for high $C(t)$, matching *GNW* ignition and recurrent processing dependencies (1, 2, 4, 6-8, 22). In line with perturbational complexity measurements, $C(t)$ covaries with integrated, differentiated neurodynamics measurable by Perturbational Complexity Index (*PCI*)(73). Therefore, access to

consciousness requires both broad neural activation and two-way neurocoherence.

Predictive Coding Energy and Conscious Access

The emergence of large-scale neural synchronization provides a neurodynamical substrate for interareal neurocommunication. Functionally, such coordinated activity supports hierarchical inference processes, as described by predictive coding frameworks. In this view, cortical neurodynamics can be interpreted as

minimizing prediction errors through reciprocal interactions between feedforward and neurofeedback pathways. Predictive coding posits that hierarchical cortex minimizes a precision-weighted prediction-error functional (11, 17, 80). Let r_l denote the representation at layer l and μ_l its top-down prediction. Then, the prediction error is,

$$e_l = r_l - \mu_l,$$

and the global energy is given by the optimization principle of error minimization via hierarchy, i.e.

$$E = \sum_l \|e_l\|^2_{\Sigma_l^{-1}},$$

where Σ_l is the error covariance (precision Σ_l^{-1}). Gradient descent on E yields canonical microcircuit neurodynamics for exchanging predictions and errors such that superficial neural populations encode errors; deep populations carry predictions (11, 17, 80), i.e.

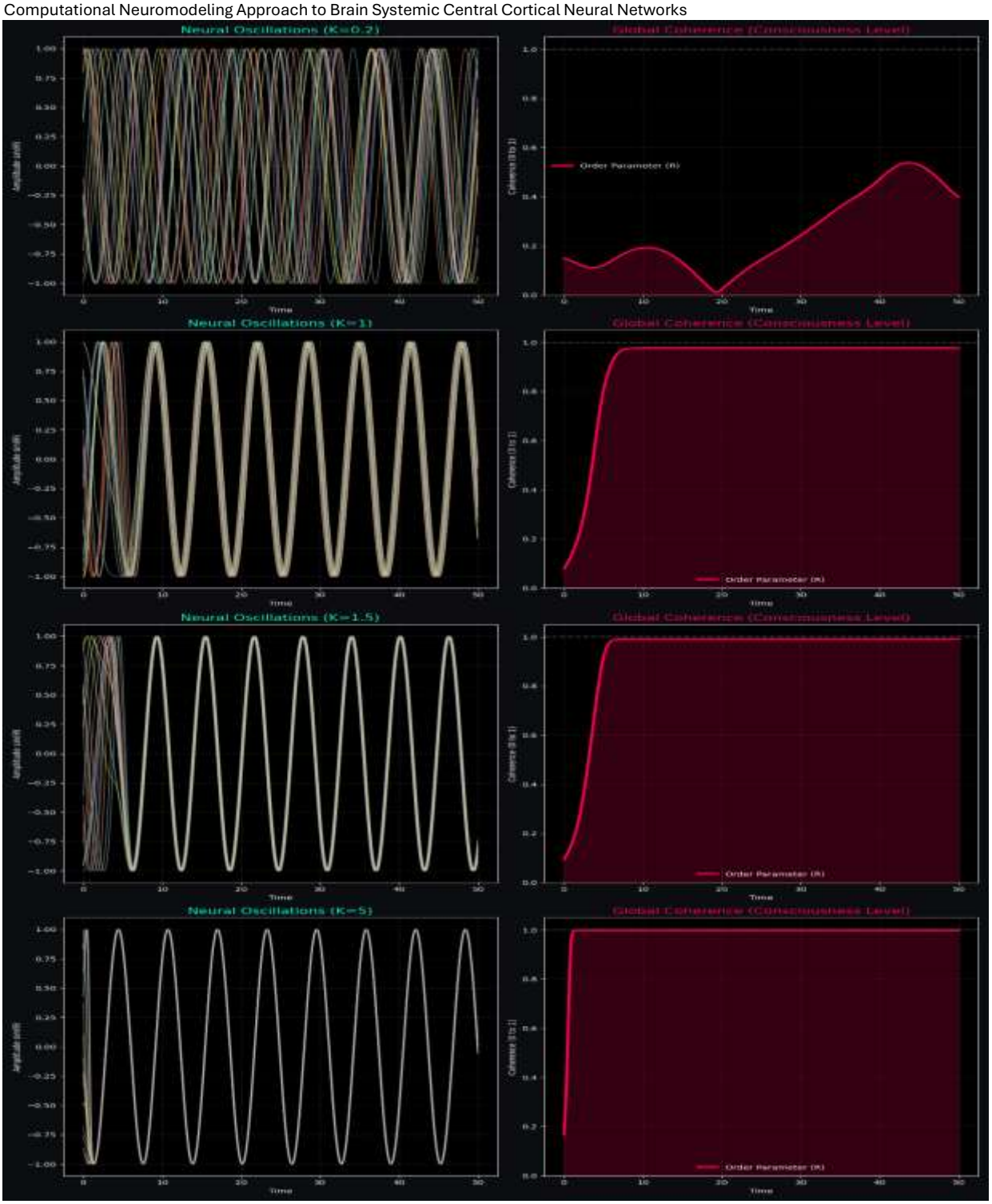


Fig. 6. The Computational Model of Kuramoto Neurocoupling. Neurooscillations (Left): The waves that were scattered at the beginning, slowly start to shoot into the peaks (Phase-Locking). **Order Parameter**

***R* (Right):** When *R* jumps close to 1.0, that is the moment when the system becomes a supersystem. It is a computational representation of the transition from unconscious to conscious neural processing. Neurocoupling *K* parameter is given for K = 0.2. K = 1, K = 1.5, and K = 5.0 (from **Top to Down**). For lower values of *K* the synchronization disappears (chaos). Cranking it up to 5.0 gives almost instant Conscious Ignition.

$$\frac{dl}{dt} \propto -\frac{\partial E}{\partial r_l} = -\Sigma_l^{-1} e_l + W_{ff}^T \Sigma_{l-1}^{-1} e_{l-1} - W_{fb} \Sigma_{l+1}^{-1} e_{l+1}$$

W_{ff}, W_{fb} are feedforward and neurofeedback of the projective matrix, respectively. First member gives local correction, second/third is error propagation down/up the hierarchy. Conscious access then corresponds to a regime in which E is sufficiently suppressed across a large, distributed set of layers while activity remains high, an energetic flat valley combined with ignition. We formalize $C(t)$ with two conditions:
A global activity criterion:

$$\alpha^T x(t) > \theta_c.$$

A prediction-error criterion:

$$E(t) < \epsilon_c.$$

Thus, we have

$$C(t) = \sigma(\epsilon_c - E)\sigma(\alpha^T x - \theta_c),$$

where ϵ_c is the total error (consistency) threshold. The condition product requires both broad activation and low residual error. This formalizes the stabilized interpretation as an access condition. This resolves an apparent paradox: conscious content is both widespread (high activation) and internally consistent (low error), consistent with late stabilizations observed in *MEG*/*EEG* (2, 4, 46). As empirically observed, the laminar spectral separation supports prediction passing via alpha/beta and error broadcasting via gamma wave pattern (22).

General Neurostructural and Functional Neural Network Mapping

While predictive coding characterizes the neurofunctional objective of cortical neuroprocessing, it does not fully specify the representational and associative structure underlying neural computations. To address this, we introduce a complementary neuroarchitectural framework combining neurotopographic feature mapping and attractor-based associative memory. Our neocortical computational neuromodel comprises combined supersystemic Kohonen-Hopfield neural network. Kohonen cortical neural network represents neurotopological presentational part of the general network model enabling somatotopic, tonotopic and retinotopic neuromapping of perceived stimuli representing the external world (**Fig. 8**). It gives a presentational picture of reality by mapping its features while Hopfield associative neural network processes, combines and integrates this representation into a conscious mind content and awareness about that same reality. We model cortical neuromicrocolumns as the neural units of a cortical Kohonen neuromap whose neurosynaptic weights encode feature prototypes, i.e. we treat each cortical neuromicrocolumn as a single cortical neuroensemble carrying a unit neural function in the network. Thus, in this computational network model, analogously to classical neurons, the fundamental neurocomputational units are now cortical neuromicrocolumns, not individual neurons themselves. These neuromicrocolumns simultaneously serve as

nodes of the Kohonen *SOM* and as recurrent units of the Hopfield associative memory. Cortical laminar neural recurrent neuromicrocircuits within and across the cortical neuromicrocolumns implement classical, neurally encoded Hopfield associative memory (11, 16, 19, 32-34). Let's take a (neo)cortical Kohonen *SOM 2D* neurotopological grid consisting of M neural map neuromicrocolumnar units, each with fixed, unique positional coordinates $\boldsymbol{r}_i$ ($\mathbb{R}^2$) in the cortical sheet coordinate system of the grid, and internal inter-neuronal connection synaptic weighs $\boldsymbol{w}_i$ in a *D*-dimensional feature space ($\mathbb{R}^D$). Let N denote the number of neural recurrent units for the corresponding Hopfield neurodynamics; practically, N may be equal to M if we index a single neuromicrocolumn

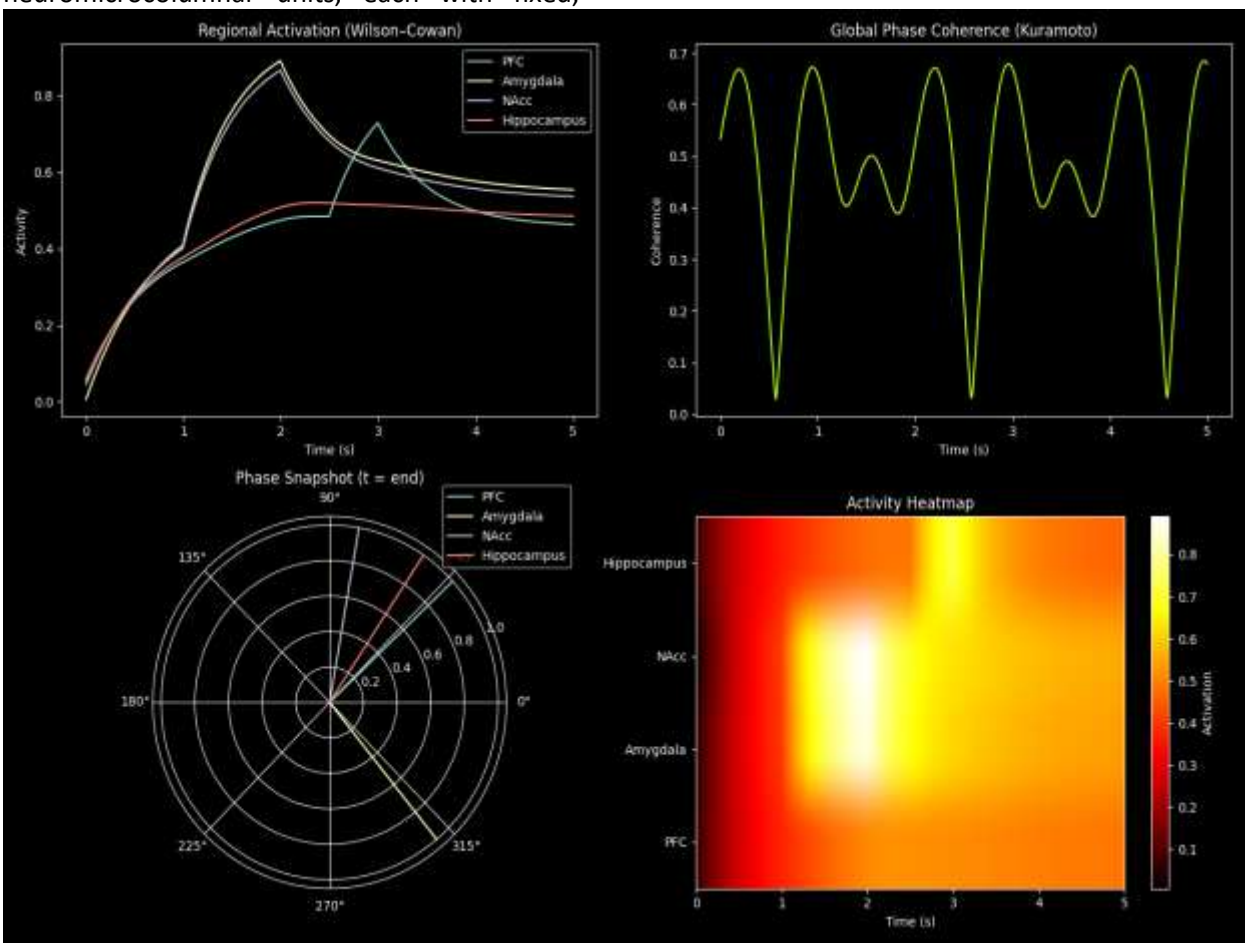


Fig. 7. Simulated Neurodynamic Model of Emotional Neural Processing and Network Synchronization (Combined Wilson-Cowan-Kuramoto Neuromodel and Limbic/*PFC* Neurodynamics). The simulation illustrates how spatially distributed regional brain neurodynamics and large-scale neural synchronization may jointly contribute to temporally evolving emotional states through which emotionally salient information biases cortical *PFC* attractor stabilization and conscious access. **(Top Left)** Simulated regional activation neurodynamics based on a Wilson–Cowan framework across key emotion-related brain regions, including the prefrontal cortex (*PFC*), amygdala, nucleus accumbens (*NAcc*), and

hippocampus. Regional neuroactivity evolves over time under coupled excitatory–inhibitory neurodynamics, exhibiting transient activation peaks followed by stabilization. **(Top Right)** Global phase coherence modeled using a Kuramoto synchronization framework, illustrating neurodynamic fluctuations in large-scale network synchrony potentially associated with transient emotional integration. **(Down Left)** Final phase snapshot of regional neurosynchronization states, demonstrating relative phase organization among simulated brain regions at the end of the temporal evolution. **(Down Right)** Activity heatmap showing temporally evolving activation intensity across brain regions, highlighting transient limbic amplification and gradual network stabilization.

neuronal population, or N can equally index a spatially distributed neuroensemble, in general. The crucial aspect is that recurrent neurosynaptic coupling is shaped by neurotopographic distance between neuromicrocolumnar nodes of the cortical Hopfield network, consistent with short-range horizontal neural connections implemented by a real neurobiological classical associative Hopfield neural network in contrast to the corresponding theoretical, artificial, fully connected model (16, 33), i.e.,



Fig. 8. Kohonen *SOM*. Top Left (Epoch 0): This is Initial Chaos. The brain receives stimuli, but has no idea where it belongs. There is no correlation. Intermediate stages (100, 400): The flecks of color come together. Neurons begin to communicate with their neighbors and agree on who will react to what (Neighborhood Function). **Bottom Right** (Epoch 1000): Perfectly edited neuromap. Similar colors are adjacent to each other (stable neurotopographical representation, like the primary visual cortex).

$$J_{ij} = J_0 exp\left(-\frac{\|\boldsymbol{r}_i - \boldsymbol{r}_j\|^2}{2\sigma^2(s)}\right),$$

where, J_{ij} is a Gaussian determined neuroconnection weight between two cortical neuromicrocolumnar nodes of the cortical recurrent Hopfield neural network, and J_0 is the strongest possible neuroconnection between them.

Kohonen SOM Formalism and Cortical Neurotopographic Classical Neural Information Encoding and Representation

Given a thalamocortical or cortico-cortical sensory neural input $\boldsymbol{x}$ in encoding feature space $\mathbb{R}^D$, the best matching unit (*BMU*) of a cortical neuromicrocolumnar Kohonen *SOM* that is the best in a neuromapping task of central cortical input representation is

$$j = \arg min_i \|\boldsymbol{x} - \boldsymbol{w}_i\|,$$

where prototype $\boldsymbol{w}_i$ vector approximates the local center of the neural input distribution $P(\boldsymbol{x})$. The Euclidean norm is a measure of the similarity of the input $\boldsymbol{x}$ and prototype $\boldsymbol{w}_i$, j is the index of the neuromicrocolumnar unit whose prototype is closest to the target, input one and therefore defines the *BMU* winner in the neuromapping process. The *BMU* choice sets a neurotopologically grounded coordinate support (reference unit) for neuroplasticity and activation in the Kohonen neuromap. Let the interneurocolumnar neighborhood function be Gaussian,

$$h_{ij}(t_s) = exp\left(-\frac{\|\boldsymbol{r_i} - \boldsymbol{r_j}\|^2}{2\sigma^2(t_s)}\right),$$

where t_s is a discretized time step and $\sigma(t_s) > 0$ is the radius (width) of the neighborhood that decays with learning epochs s; it implements network annealing. $\boldsymbol{r}_i$ is the *BMU* coordinate vector of a neuromicrocolumnar unit i, $0 \leq h_{ij} \leq 1$ gives the strength of neural neighborhood neuromodulation of neuroplasticity/unit neuroactivation conditioned by distance from the *BMU*. This describes local-lateral inter-neuronal interaction in a neurotopology-preserving map where closer units learn/activate more. In this neural model the standard *SOM* learning weight update is given by the following law,

$$\boldsymbol{w}_j(t_s + 1) = \boldsymbol{w}_j(t_s) + \alpha(t_s)h_{ij}(t_s)\left[\boldsymbol{x} - \boldsymbol{w}_j(t_s)\right],$$

where $0 \leq \alpha(t_s) \leq 1$ represents a learning rate for the slowly decaying *SOM* at epoch t_s satisfying Robbins–Monro algorithmic rules (36, 39, 86),

$$\alpha(s) \to 0, \quad \sum_s \alpha(t_s) = \infty, \quad \sum_s \alpha^2(t_s) < \infty.$$

The difference $\boldsymbol{x} - \boldsymbol{w}_j(t_s)$ represents a prototype error relative to input, so-called correction vector. We can see that h_{ij} enables and in some way represents a contribution of an i-th unit to $\boldsymbol{w}_j$ in every learning iteration. Giving the gradient shift of prototype towards input proportional to neurotopological proximity and learning rate, this update rule ensures correct and organized feature neural mapping and central neocortical input representation. Under these conditions, with mild assumptions on input distribution $P(\boldsymbol{x})$ and annealing of σ, the weights converge to a neurotopologically ordered neural code approximating $P(x)$ (39, 86). The activation neural vector component $a_i(x)$ of a neurocolumnar unit is defined by

$$a_i(x) = h_{ij}(t_s),$$

where a_i is the neurotopological single activation level of a particular neurocolumnar unit node of the network defined exclusively by the neighborhood around the *BMU*, or by a graded similarity we have the corresponding Gaussian behaviour of a neurocolumnar activation output

$$a_i = exp\left(-\frac{\|\boldsymbol{x} - \boldsymbol{w}_i\|^2}{2\sigma_a^2}\right),$$

where $\sigma_a > 0$ is the width parameter of the Gaussian similarity function in the feature space. This gives us a smooth, metric-driven activation based on the similar roles of h_{ij} and $\boldsymbol{w}_i$, i.e. two complementary metric activations – one topological, on the map and the other in the feature space. Therefore, we have a neurotopographic, low-dimensional embedding that preserves neighborhood relations in input space, consistent with retinotopy, tonotopy, and somatotopy (87, 88).

Hopfield Neural Formalism and Cortical Network Attractor Stability

The Kohonen *SOM* provides a neurotopographic embedding of sensory inputs, preserving similarity relationships in cortical space. However, neurotopographic representation alone does not account for the neurointegration and stabilization of distributed neural activity patterns. This role is naturally fulfilled by recurrent associative neurodynamics, which we model using a Hopfield-type network (**Figs. 9, 10**). Let $\boldsymbol{q}$, being a neural activation binary state vector of a neocortical Kohonen *SOM* associated neuromicrocolumnar recurrent Hopfield associative neural network and given by N neurorecurrences, is defined as

$$\boldsymbol{q} \equiv \{-1, +1\}^{N},$$



Fig. 9. The Recognition Process of a Classical-Holographic Hopfield Associative Neural Network Neurodynamics. Network Convergence: (from **Left to Right**) The image cleans up (so-called associative recall). The network recognizes the pattern due to the classical neuroholographic memory storage principle even though it was partially destroyed.

where $\{-1, +1\}$ represents binary representation of cortical neuromicrocolumnar Hopfield neurorecurrent unit activation states in Ising formalism with modalities active ($q_i = +1$)/inactive ($q_i = -1$) given formally as components of the neuroactivation state vector $\boldsymbol{q}$. Then, the classical Hopfield neural network state vector $\boldsymbol{q}$ describes the configuration of the global attractor state that the network stabilizes. With symmetric weights of cortical Hopfield interneuromicrocolumnar connections

$$w_{ij} = w_{ji}$$

and no self-coupling $w_{ii} = 0$, the local field f_i determining the cumulative recurrent contribution-based update of q_i is given by

$$f_i = \sum_j w_{ij}\, q_j + b_i,$$

where f_i is a local input field of an i-th neuron. It represents neurocomputational model analog to neurobiological postsynaptic local potentials, excitatory (*EPSP*) and inhibitory (*IPSP*) in a neurocybernetic model of the network. q_j is the neuroactivation state of a neuromicrocolumnar Hopfield network node and b_i gives a local bias that includes top-down and contextual influences. Asynchronous updates (one network node at a time) of $\boldsymbol{q}$ on the other hand obey the following deterministic rule for choosing a stable output sign according to the local field, i.e.

$$q_i \leftarrow sig(f_i),$$

where the signum function $sig(f_i)$ returns +1 if $f_i \geq 0$ and −1 otherwise. Asynchronous update guarantees a monotonic energy decay. The Hopfield energy is given by

$$E_H(\boldsymbol{q}) = -\frac{1}{2}\boldsymbol{q}^T \boldsymbol{W}\boldsymbol{q} - \boldsymbol{b}^T\boldsymbol{q},$$

where $E_H(\boldsymbol{q})$ is a Lyapunov function (**Fig. 11**) under asynchronous updates ($\Delta E_H \leq 0$ for single spin flips), global scalar description of the depth of the attractor landscape ensuring convergence to a local minimum (35, 38), $\boldsymbol{q}^T \boldsymbol{W} \boldsymbol{q}$ is a quadratic form that rewards consistent co-activations by weight $\boldsymbol{W}$, $\boldsymbol{b}^T \boldsymbol{q}$ represents a linear bias that tilts the attractor landscape towards pre-favored configurations. The factor 1/2 avoids double counting of (i, j) pairs. Since asynchronous updates do not increase E_H, convergence to local minima is ensured. Patterns of neural network activity $\xi^{\mu} \equiv \{-1, +1\},^{N}$ are stored via Hebbian correlation learning that encodes associations into a symmetric neurosynaptic weight matrix,

$$\boldsymbol{W}_{ij} = \frac{1}{N} \sum_{\mu=1}^{P} \xi_i^{\mu} \, \xi_j^{\mu},$$

where, $\xi^{\mu} \equiv \{-1, +1\}^{N}$ is the μ-th memorized pattern, P is the number of patterns. For random uncorrelated patterns, the classical Hopfield network supporting associative recall exhibits a critical storage up to a capacity of $P \approx 0.138\, N$, (with $w_{ii} = 0$), corresponding to a critical load $\alpha_c = P/N \approx 0.138$ (13-14%) (38). In neurobiologically structured cortical neural networks with neurotopographic constraints and correlated patterns, this value represents a conservative lower bound rather than a strict limit. Modern variants allow superlinear capacities and continuous states (37, 89, 90).

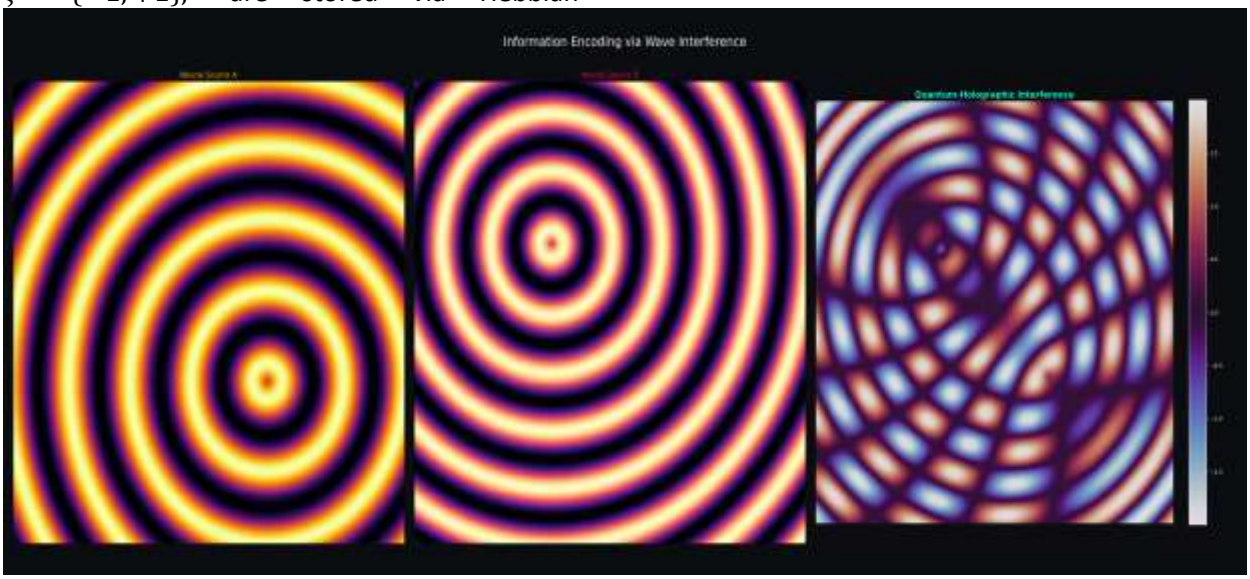


Fig. 10. ***CA-SOM*** **Neurohology Principle. Neuroholographic Memory: (Far Most Right)** Complex pattern is obtained, which is not a simple sum of *A* (**Far Most Left**) and *B* **(Middle)**, but a new code. At macroscale, this is what Raković refers to as the Quantum-Neuroholographic Framework, i.e. so-called macroscopization of brain quantum phenomena to the entire mind-body level of the hierarchical organization, which that way represents one of the modern solutions to the great and famous Mind-Body Problem, by the way, and in parallel reflects acupuncture system as an implementor of the framework. **Non-Locality:** Cutting a piece of this hologram, it still contains information about the whole complying that way to the general principle of holography.

$1/N$ is a normalization factor that keeps fields of order $O(1)$ as $N \to \infty$.

Neurotopographically Biased Associative Memory

To reflect cortical neuroconnectivity favoring short-range lateral neuroconnections, we shape $\boldsymbol{W}$ by *SOM* distances. Let $\boldsymbol{r}_i$ be the *SOM* coordinate of a neural unit i, and define a Gaussian neurotopographic kernel K_{ij} as

$$K_{ij} = exp\left(-\frac{\|\boldsymbol{r}_i - \boldsymbol{r}_j\|^2}{2\sigma_w^2}\right).$$

Synaptic weights of the cortical Hopfield associative neural network (**Figs. 9, 10**) are represented by a neurotopographically weighted Hebbian,

$$w_{ij} = \frac{1}{N}\sum_{\mu=1}^{P} K_{ij}\xi_i^{\mu}\,\xi_j^{\mu}, \qquad w_{ii} = 0,$$

where $0 \le K_{ij} \le 1$ represents neurotopographic kernel that monotonically decreases with cortical distance $\|\boldsymbol{r}_i - \boldsymbol{r}_j\|$. It modifies standard Hebbian learning to favor short-range neurorecurrence, consistent with neocortical structure. Therefore, this Hebbian implements dense local and sparse long-range neuroconnectivity. Neurally stored information patterns are not arbitrary vectors but respect cortical neurotopology. Neurocoupling strength decays with physical, neurofunctional distance. This implements the experimental constraint on dense local neurorecurrence and sparser long-range neuroconnections (16, 33).

CA-SOM Energy and Neurodynamics

To now unify neurotopographic representation and associative neurointegration, we go even further and couple the Kohonen *SOM* with Hopfield neurodynamics into a composite energy-based cortical neural system model (**Fig. 12**). This combined neuroarchitecture enables the network to simultaneously encode sensory

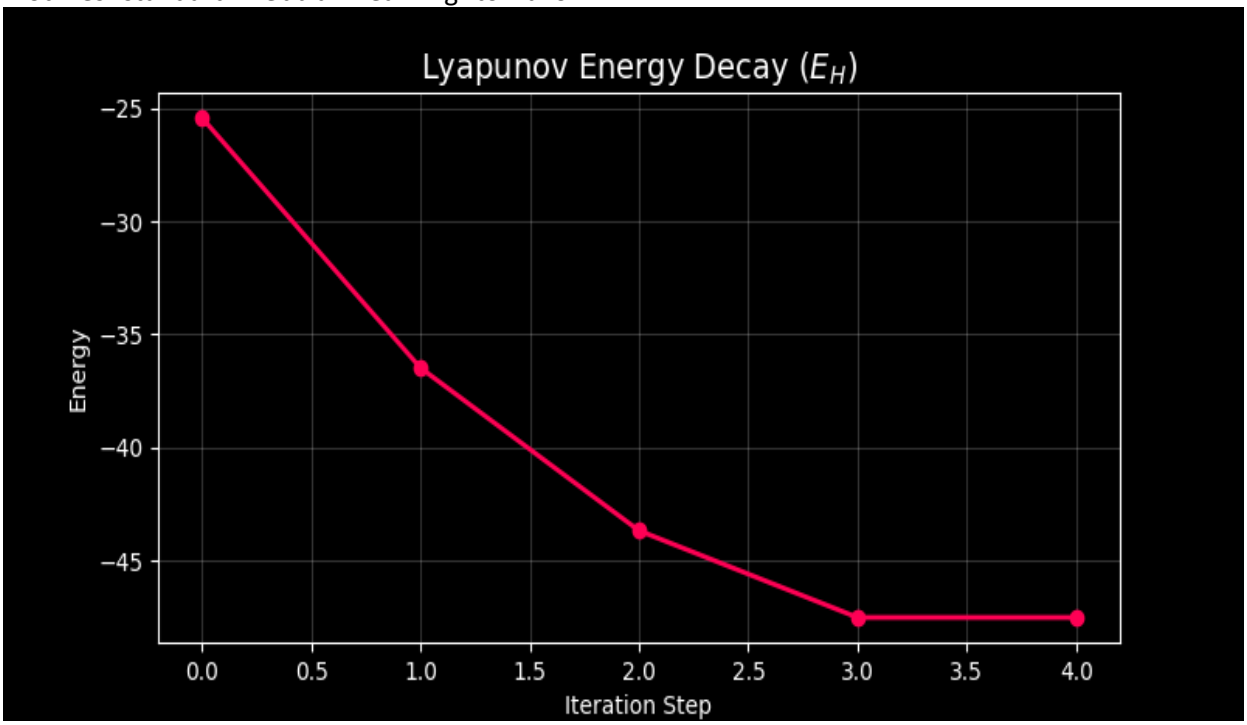


Fig. 11. Lyapunov Energy Decay. Classical Hopfield network energy neurodynamics during cortical attractor creation process. Stable consciousness attractors have lower energy content (Energy Minimum in a System Cortical Network Energy-Configurational Hypersurface).

structure and converge to stable, globally consistent attractor states, reflecting coherent conscious content. We define a composite energy E_c that couples Hopfield stabilization with a neurotopographic match-to-input term given by

$$E_c(s|x,m) = E_H(s) + \lambda E_{SOM}(s|x,m),$$

where E_c is the total energy that couples the stability of the associative Hopfield attractor to the topographic neural input fit and $\lambda > 0$ being a coupling parameter (so-called coupling constant) that balances the Hopfield and *SOM* criteria. This gives a unique energy landscape in which attractors favor both memorized patterns and current sensory input. We specify E_{SOM} as a mismatch weighted by current neural activity,

$$E_{SOM}(s|x,w) = \frac{1}{2}\sum_j s_j^2\, h_{ij} \left\|\boldsymbol{x} - \boldsymbol{w}_j\right\|^2,$$

where s_j^2 gives an emphasized, weighted representation of nodes contributing to the current content (for binary states $s_j^2 = 1$), $\left\|\boldsymbol{x} - \boldsymbol{w}_j\right\|^2$ is a squared error between input and prototype unit j, h_{ij} Gaussian neighborhood factor around i-th *BMU* (the h_{ij} term focuses the mismatch around the *BMU* neighborhood for binary states). The factor 1/2 is a conventional squared error normalization. E_{SOM} penalizes the activation of nodes whose prototypes do not match the input, especially around the *BMU*. For one Hopfield spin flip at i, we have

$$\Delta E_H = -(q_i' - q_i)\sum_j W_{ij}\, q_j + b_i,$$

where $q_i' - q_i \equiv \{-2,0,2\}$ is a change of spin i, a sum term is a local field f_i. A negative product guarantees no increase in energy during a correct flip. This gives Lyapunov monotonicity (monotone descent) under asynchronous update $q_i' \leftarrow sig(h_i)$. For binary q, we have $q_i'^2 - q_i^2 \Longrightarrow \Delta E_{SOM} = 0$, thus $\Delta E_{SOM} = 0$ and therefore $\Delta E_C \leq 0$ for spin flips. Since $q_i^2 = 1$, flip does not change E_{SOM}. Thus, the *SOM* criterion does not violate the convergence of

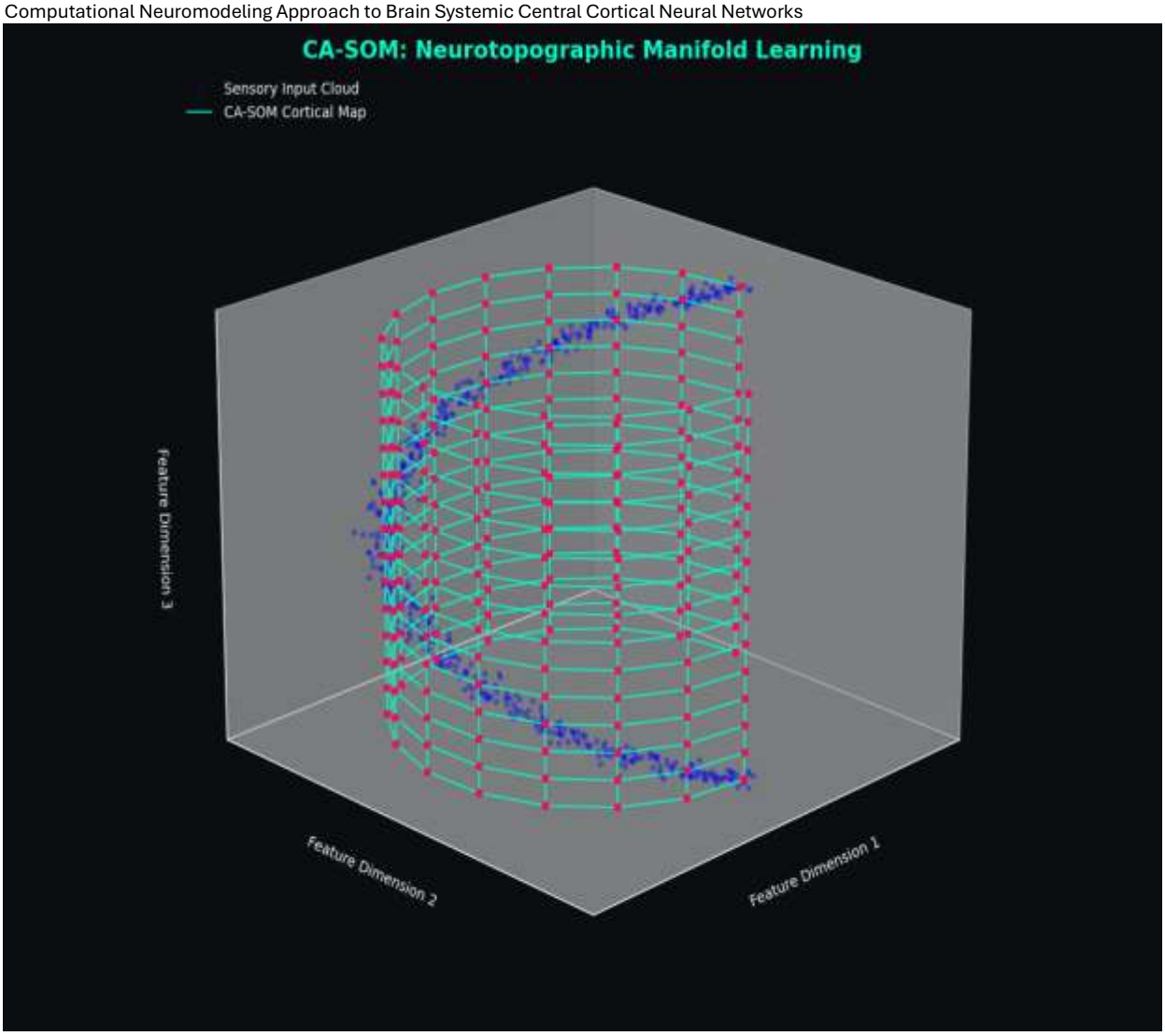


Fig. 12. CA-SOM Manifold Learning. Neurotopological Conservation: The system cortical neural network maintains its neuroconnectivity (neighboring neurons remain adjacent), but changes shape in 3D space to understand the structure of the data, so-called Neurotopography. **Cortical Neuromicrocolumns:** The red dots are neurofunctional units. They are clustered where there is the most data, optimizing brain resources. **Dimensionality Reduction:** Even though the data is modeled in 3D (or of order ~10^3D in reality), the *CA-SOM* neuromodel maps it to the 2D surface of the cortex without losing its essence.

the Hopfield part at binary states. For graded s with continuous-time neurodynamics,

$$\frac{ds}{dt} = \frac{\partial E_C}{\partial s},$$

energy descent is immediate. $s \equiv \mathbb{R}^N$ allows continuous-saturation of network nodes, $\frac{\partial E_C}{\partial s}$ gives the fastest, steepest descent in the energy landscape. It immediately ensures a monotonous decrease of E_c in the continuum.

Thus, with fast s-updates and frozen w, the coupled system decreases E_c until a stable state is reached. The neurotopographic mismatch does not impede Hopfield convergence but shapes the attractor basins via λ and h_{ij}, funneling neural network neurodynamics toward states that both match stored associations and are consistent with current cortical input neurotopology (**Fig. 13**).

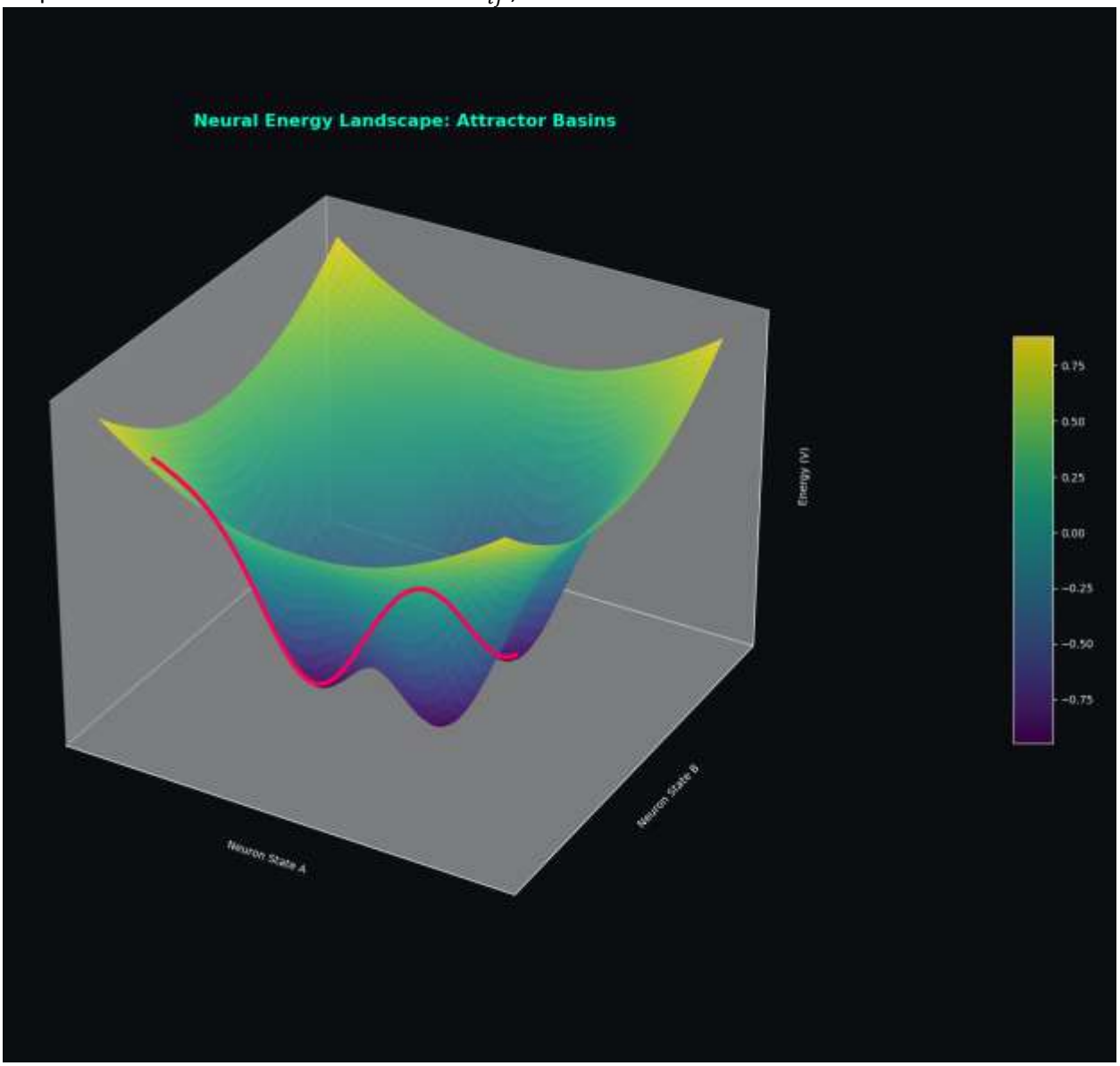


Fig. 13. The Cortical Attractor Landscape of a Network Energy-Configurational Hypersurface. Basins of Attraction: Each hole on the graph is one memorized content. When the *CA-SOM* recognizes an entrance, it slides into the nearest attractor (graph landscape hole). **Path (Red Line):** It is a process of thinking or recognizing. The system starts from chaos (the edge) and gravitates towards stability (the center of the hole). **Meta-stability:** If the landscape is flat, consciousness is chaotic. If the holes are too

deep, the system is rigid (e.g. obsessive thoughts). A healthy consciousness is a balance, i.e. a metastable landscape where it is easy to move from one valley to another.

Multi-Timescale Stability

The coupled neural system naturally operates across multiple timescales: fast recurrent dynamics drive rapid convergence to attractor states, while slower neuroplastic processes reshape the underlying representational landscape. This separation of timescales ensures both stability and adaptability of cortical processing. We assign slow timescale to *SOM* learning $m(s)$ and fast timescale to Hopfield states $s(t)$. For fixed m and x, $s(t)$ converges to $s^*(x,m)$ minimizing E_C. Across learning epochs, $m(s)$ updates by the *SOM* rule with learning rate $\alpha(s)$ satisfying Robbins–Monro condition (39, 86). This yields a singular perturbation or quasi-static separation - fast convergence to s^* conditional on slowly varying m. Slow adaptation of m shapes future attractor basins under standard assumptions of multiscalar Robbins–Monro convergence condition. The first step becomes small at the stabilization stage, the second represents sufficient overall shift (consistency) and the third is variance control where convergence is almost certain. This enables quasi-static separation, i.e. fast $s(t)$ follows minima while slow $m(s)$ adapts. For bounded inputs and symmetric W the joint system converges. The slow variable sees the fast subsystem stabilized, the fast subsystem continuously tracks near-equilibria as m evolves (86, 91).

Information-Theoretic Alignment

The interaction between fast attractor neurodynamics and slow representational adaptation can be further understood from an information-theoretic perspective. In particular, the alignment between neurotopographic representations and attractor states increases the shared statistical structure within the neural system, providing a quantitative proxy for neurointegration. Let $H = s^*(X)$ denote the Hopfield attractor state and $S = a(X)$ the *SOM* neuroactivation pattern, viewed as random variables induced by the input distribution $P(X)$. We define a mutual information proxy $I(H;S)$ computed over $P(X)$. Because the coupling energy E_C aligns the Hopfield state with the neurotopographic representation of the input and stored associations, training tends to increase statistical dependence between H and S. From a variational expectation–maximization perspective, minimizing the expected coupling energy $\mathbb{E}_{P(x)}[E_C(s|x)]$ encourages alignment between features selected by the *SOM* and attractors retrieved by the Hopfield layer $s^*(X)$, which is expected to increase $I(H;S)$ under bounded entropy constraints (5, 92). Thus, unity (integration) can be interpreted as the maximization of shared structure between a neurotopographic code and a global attractor, consistent with the integration requirement of *IIT* in a proxy form (5, 10).

Oscillatory Neuromodulation and Neural Binding

Beyond static measures of neurointegration, cortical neuroprocessing is inherently neurodynamic, with neurooscillations modulating effective neuroconnectivity over time. These neurooscillations provide a mechanism for temporal coordination and selective routing of information across neuroassemblies. Cortical neurooscillations modulate effective neuroconnectivity and communication-through-neurocoherence (42, 44). We incorporate neurooscillatory gain which gives rhythmic enhancement of effective

neuroconnectivity/threshold in accordance with neural rhythms

$$g(t) = 1 + \rho \cos(\omega t + \phi),$$

where $0 \leq \rho \leq 1$ is gain neuromodulation amplitude, ω angular frequency of the neurooscillatory mode (e.g. gamma, beta), ϕ phase shift into thresholds or recurrent gains,

$$h_i \leftarrow g(t) \sum_j W_{ij}\, q_j + b_i,$$

where $g(t)$ multiplies the recurrent part; b_i remains additive bias. Thus, phase-matched circuits get a higher effective synaptic weight. Phase alignment between neuroensembles encoding related features increases effective W_{ij} by temporal gating, which tightens attractor basins and speeds neuroconvergence (6, 41-44). Layer- and frequency-specific channels (e.g., gamma feedforward; beta feedback) can be integrated by letting σ_W or λ be frequency-modulated (41). The result is a neurodynamical binding mechanism that sits atop the energy-based convergence, consistent with observed rhythms during conscious processing (6, 41-44, 69).

Significance of Cortical Neuroarchitectonics

Taken together, these mechanisms, from biophysical neurodynamics to large-scale network organization and information-theoretic integration, form a coherent theoretical framework in which conscious access emerges as a neurodynamical, multi-scale phenomenon grounded in cortical neuroarchitecture. First, minicolumnar neuromodularity yields discrete units with local circuitry (*SOM* neurons), enabling neurotopographic mapping of features (32, 34, 87). Laminar recurrent loops supply Hopfield attractor stabilization, with short-range lateral neuroconnections shaping the energy geometry (11, 16, 19, 33). Long-range neurofeedback between higher and lower areas supplies top-down bias terms and modulation of $\sigma(s)$, bridging predictive coding and workspace broadcasting (2, 9, 11, 28, 68-72). Neurooscillations gate effective connectivity and enhance integration through phase alignment (6, 41-44). Together, these ingredients satisfy the joint requirements for classical neural consciousness: (i) composition (map structure), (ii) information (specific feature (en)coding), (iii) neurointegration (attractor unity), (iv) exclusion (winner-take-all minima), and (v) intrinsic existence (realized by internal causal neurodynamics) (2, 4, 5, 8-10).

The Classical Limit of Consciousness

Open Quantum Systems and the Lindblad Master Equation

Because microscopic quantum degrees of freedom in brain tissue are inevitably embedded in an open and thermally noisy environment, any putative quantum substrate of consciousness must first be described as an open quantum system subject to quantum decoherence. Thus, any particular microscopic quantum degrees of freedom in central neural tissue, e.g., electron or nuclear spins, vibrational modes, or putative neuronal microtubule excitations, exist as open quantum systems coupled to a large thermal environment with quantum density operator $\rho(t)$ obeying the Lindblad master equation (47, 48):

$$\frac{d\rho}{dt} = \sum_k \left(L_k \rho L_k^\dagger - \frac{1}{2}\{L_k^\dagger L_k, \rho\} \right) - \frac{i}{\hbar}[H, \rho],$$

where H is the system Hamiltonian and L_k are Lindblad operators encoding system–environment coupling. In the brain's warm, wet and noisy neurobiological conditions, the coupling is strong and Markovian approximations usually hold, leading to rapid quantum decoherence and effective classicality in the relevant basis, often position for massive degrees of freedom (13, 31, 47, 48).

Quantum Consciousness and Spontaneous Symmetry Breaking

Although quantum decoherence rapidly suppresses many quantum correlations, *QFT* still provides mechanisms through which collective quantum organization may transiently emerge before classical reduction. One such mechanism is spontaneous symmetry breaking (*SSB*) (**Fig. 14**). Spontaneously broken neuroquantum field symmetry generates Nambu–Goldstone modes with long-range correlation, so-called collective modes. Consider a hypothetical complex scalar field $\Phi(x,t)$ representing coherent microstructural degrees of freedom (for instance, collective dipole modes in cytoskeletal assemblies). We define a Lagrangian density,

$$\mathcal{L} = (\partial^{\mu}\Phi)\left(\partial_{\mu}\Phi\right) - V(|\Phi|^2),$$

with

$$V(|\Phi|^2) = \lambda(|\Phi|^2 - \eta^2)^2,$$

where $\Phi(x,t)$ is a complex scalar field, $\left|\partial_{\mu}\Phi\right|^2$ is a kinetic term (space-time field changes), V is Mexican-hat potential, $\eta > 0$ sets the vacuum modulus and $\lambda > 0$ is the strength of the nonlinearity of the potential. $\mathcal{L}$ has a degenerate Mexican-hat minimum at $|\Phi| = \eta$. *SSB* selects a phase $\theta(x)$ and amplitude approximately equal to η; the low-energy excitations are massless Nambu–Goldstone boson collective modes $\theta(x)$ and a massive radial mode $\sigma(x)$ (58, 63). Long-range correlations in $\theta(x)$ can, in principle, coordinate classical degrees of freedom via effective fields (56, 63, 64). This construction is a standard *QFT* mechanism without presupposing any particular biology.

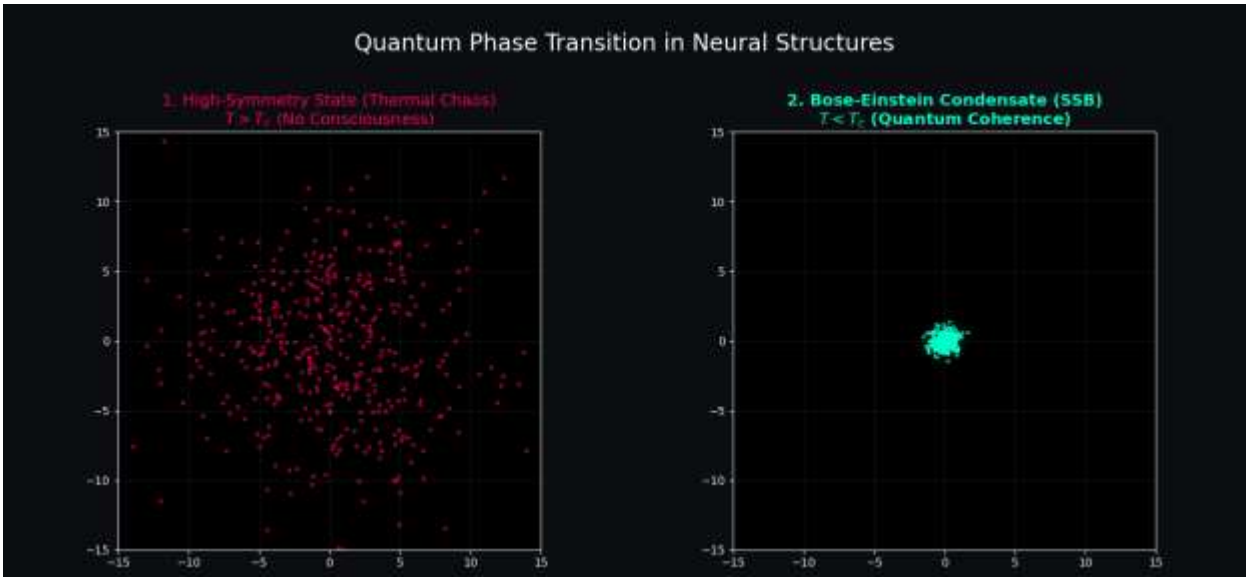


Fig. 14. Brain *SSB-NGBCM* Fröhlich Condensate. This model simulates how neuronal microtubules or neuromembranes enter into coherent vibrations. **Phase Transition:** Visually shows the transition from disordered to settled state. It is quantum consciousness that is born out of neurobiological chaos. ***SSB-NGBCM*: (Left)** The particles can be anywhere (full symmetry). **(Right)** The system picked the center. It is the moment when vagueness turns into a concrete conscious state.

Parisi–Wu Stochastic Quantization and Langevin Neurodynamics

If such collective quantum field configurations actually exist, a theoretical bridge is then needed to connect microscopic quantum-field distributions to effective stochastic neurodynamics. Stochastic quantization offers one such formal route. Parisi–Wu stochastic quantization formalizes a path from quantum field distributions to stochastic differential equations by introducing a fictitious time τ and Langevin dynamics:

$$\frac{\partial \Phi}{\partial \tau} = -\frac{\delta S[\Phi]}{\delta \Phi} + \xi(x,\tau),$$

where τ represents fictional quantization time, not identical to physical time t. $S[\Phi]$ is Euclidean action, $\frac{\delta S[\Phi]}{\delta \Phi}$ is functional gradient (drift), ξ is Gaussian white noise with unit intensity (37). Stochastic neurodynamics converges to the measurement distribution of the path-integral with Gaussian white noise ξ of internal neurodynamic fluctuations of the consciousness field obeying

$$\langle \xi \rangle = 0 \text{ and } \langle \xi(x,\tau) | \xi(x',\tau') \rangle = 2\delta(x-x')\delta(t-t'),$$

(noise intensity). In the stationary state, the probabilities are Boltzmannian with respect to the effective energy (74-77). Physically, open quantum systems yield quantum Langevin equations and similar effective stochastic dynamics (93).

which models learning as a non-Schrödinger Langevin evolutionary factor of consciousness as an initially modeled closed (classical/quantum) system transitioning into an open one under the influence of external perturbations. As $\tau \to \infty$, the stationary distribution of Φ recovers the Euclidean path integral measure. For coarse-grained classical observables (e.g., spatial averages of θ), the

induced Fokker–Planck equation yields a Gibbs stationary distribution,

$$p(\theta) \propto -\frac{V_{eff}}{T_{eff}},$$

where θ is phase (Nambu–Goldstone) mode or reduced coordinate, V_{eff} is an effective potential after integration of fast modes and environment and T_{eff} is effective temperature

Wigner Transform and the Fokker–Planck Limit

An equivalent route to the classical limit emerges through phase-space formulations of quantum mechanics, where decoherence transforms quantum evolution into an effective stochastic neurodynamics. To connect quantum neurodynamics to classical phase space under quantum decoherence in the brain, we consider the Wigner quasi-probability phase-space function $W(x,p,t)$, the Weyl–Wigner transform of ρ. For Hamiltonians polynomial in x and p, the Moyal bracket reduces to its classic limit, the Poisson bracket, plus corrections of order $\hbar^2$ (47, 48, 76, 77, 93). Under weak nonlinearity and strong decoherence, one obtains a quantum Fokker–Planck equation for W (13, 47, 48, 76, 77, 93),

$$\frac{dW}{dt} = \{H,W\}_{PB} + \frac{\partial}{\partial p}(\gamma p W) + D_{pp}\frac{d^2W}{dp^2} + D_{xx}\frac{d^2W}{dx^2} + \cdots,$$

where $\{H,W\}_{PB}$ is the classical Poisson bracket, γ is a friction coefficient, and D-terms are diffusion coefficients determined by the bath. The Caldeira–Leggett model provides explicit forms for γ and D in high-temperature limits (13). Truncating higher-order terms yields an effective classical stochastic process described by the Langevin equations to obtain effective stochastic classical neurodynamics with

Gaussian noise satisfying fluctuation–dissipation relations (74, 75):

$$\frac{dx}{dt} = \frac{\partial H}{\partial p} + \xi_x(t),$$

$$\frac{dp}{dt} = \xi_p(t) - \frac{\partial H}{\partial x} - \gamma p,$$

where ξ_x and ξ_p are Gaussian noises with fluctuation-dissipation ratio.

Decoherence Times, Relevance to Neural Scales and Effective Classicality

The theoretical transition toward effective stochastic classicality must, however, be constrained by empirical neurophysical timescales. Tegmark estimated quantum decoherence times τ_{dec} for superpositions in neuronal contexts, finding extremely short timescales (e.g., $\leq 10^{-13}$ s for position superpositions with micron separations), orders of magnitude shorter than neural timescales (≥1 ms) (31). For nuclear spins, coherence times can be longer, and proposals exist for long-lived nuclear spin states (e.g., in phosphate molecules), but coupling from such spins to neuronal-scale membrane potentials is weak and indirect, making controlled, macroscopically relevant quantum computation implausible in the absence of extraordinary shielding and error correction (66). In physically realistic brain conditions, any neuroquantum dynamics reduce to classical stochastic effective contributions at the scale of neurons and neuroensembles (13, 31, 47, 48). Any quantum substrate must decohere extremely fast at body temperature (31). Quantum decoherence theory shows that environmental coupling rapidly suppresses off-diagonal terms in the density matrix, selecting pointer states and yielding classical stochastic dynamics for macroscopic observables (65). Thus, rather than quantum computation, we posit that environmental coupling drives a quantum-to-classical transition where coarse variables (order parameters) evolve under effective laws governed by stochastic differential equations.

Reduction to Classical Neurodynamics

Peruš theoretically quantized neural networks by introducing the following dual, neuroquantum-classical pair of neuronal activities in a network (94-96),

$$\psi(\boldsymbol{r}, t) \Leftrightarrow \boldsymbol{q}(\boldsymbol{r}, t),$$

with quantum scale, the microscopic one implementing the quantum field aspect of neural activities of the network neurons ψ on the one side and macroscopic scale, the classical one implementing the neurophysiologically measurable voltage neuromembrane activity of the neurons $\boldsymbol{q}$ on the other, connected by the mesoscopic, semi-classical scale acting as a bridge between the two. Taking the classical neurodynamic contribution of an individual, i-th neuron to the field of consciousness, we have $\lim_{\tau\to\infty}\phi \to \boldsymbol{q}$, where $\boldsymbol{q}(\boldsymbol{r}, t; \tau)$ represents the obtained (meta)stable stationary state of the classical counterpart of consciousness. This is the classically generated, neuroemergent Bars-Franklin-McFadden's consciousness that in the classical domain has a bidirectional interaction with the brain neural network (McFaden's upload/download of consciousness to the brain) (97). That is, we get a systemic neurodynamical organization of synchronized neurocoherence that fantastically uses the existing neural resources of the Baars-Franklin's neurocybernetic model of consciousness (98, 99). By emergence, at higher organizational levels this neurodynamic construct becomes standard quantum consciousness. This stationary classical neurodynamic equilibrium is characterized by the probability distribution of neural network states,

$$P[q(\boldsymbol{r}, t)] \propto exp[-S(q)],$$

where $S(q)$ represents the formal neurodynamic quantifier of the neural network

action. This neurodynamical probabilistic distribution seems to even underlie the mental Fokker-Planck equation at the quantum-gravitational level of the consciousness system organization,

$$\frac{\partial P[\phi;\tau]}{\partial \tau} = \int d^4x \frac{\delta}{\delta\phi(x)}\left(\frac{\delta S[\phi]}{\delta\phi(x)}P[\phi;\tau] + \frac{\delta P[\phi;\tau]}{\delta\phi(x)}\right),$$

as its stationary solution for the condition,

$$\left.\frac{\partial P[\phi;\tau]}{\partial \tau}\right|_{\lim_{\tau\to\infty}\phi\to \boldsymbol{q}} = 0.$$

Thus, the $P[q(\boldsymbol{r},t)]$ represents the stable neurodynamical attractor state of the classical neural equivalent of consciousness (100). Given also the rapid decoherence constraints, we see that microscopic neuroquantum variables can only influence cortical neuroprocessing through coarse-grained effective contributions to mesoscopic neurodynamics. Let y denote a vector of classical mesoscopic neural variables (e.g., mean neuromembrane potentials, neurosynaptic currents, neuronal population rates in a neuroensembe), and ψ the Peruš's quantum microvariables. The joint neurodynamics under separation of scales can then be written as

$$\frac{dy}{dt} = f(y) + g(y, \langle O(\psi)\rangle) + noise,$$

$$\frac{d\rho}{dt} = L[\rho, y],$$

where $O(\psi)$ are quantum observables coupled to y and L is the Lindblad generator (13, 47, 48). Under rapid decoherence, ρ rapidly relaxes to a steady state conditional on y, and $\langle O(\psi)\rangle$ becomes a functional of y with added Gaussian fluctuations

$$\langle O(\psi)\rangle \approx \sigma_O(y)\zeta(t) + \bar{O}(y).$$

Substituting into y time derivative yields

$$\frac{dy}{dt} = \sigma_{eff}(y)\zeta(t) + f(y) + g\big(y, \bar{O}(y)\big),$$

i.e. a classical stochastic differential equation, where y represents mesoscopic neural variables (e.g. population rates/voltages), ψ are microquanta, $O(\psi)$ are observables that converge on y on average, $\bar{O}(y)$ is fast relaxation of the quantum subsystem to a y-dependent stationary state and $\sigma_{eff}(y)\zeta(t)$ is emergent classical noise of quantum origin. In other words, purported quantum contributions to consciousness mechanisms enter the neural equations as renormalizations of parameters and as noise sources $\sigma_{eff}(y)\zeta(t)$. This represents the classical neural limit of consciousness (**Fig. 15**). It operates according to the physical principles of content-addressable classical neuroholographic memory. Also, at this level, the perceived image is analyzed and various features of the image are extracted, which are individually encoded, so-called feature extraction.

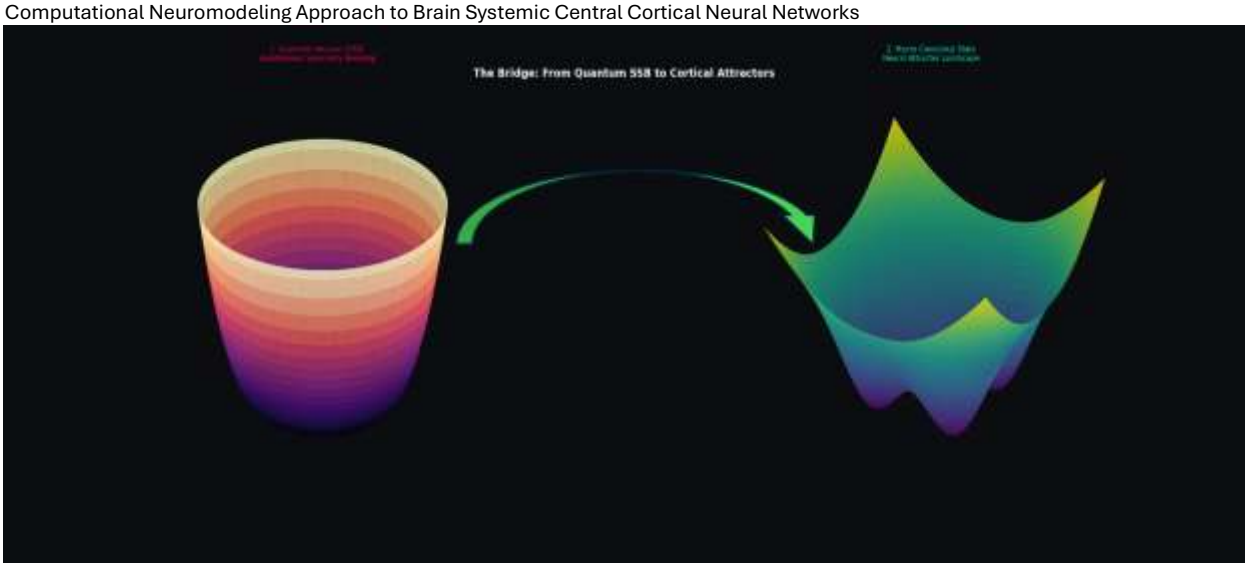


Fig. 15. The Classical Limit of Consciousness/Consciousness Neuroquantum-to Classical Neural Reduction. Neuroquantum Phenomenon **(Left):** Quantum brain Nambu-Goldstone *SSB-NGBCM* neural mechanism. The system is in neuroquantum superposition, where at this stage consciousness is still pure potential, so-called Bom's Implicate Order of Consciousness. **Actualized Brain Neurodynamics (Right):** This is realized consciousness. Neuroquantum decoherence has occurred and stable classical cortical neural attractor is created. The thought slips into one of these valleys. The cylinder from the **Left** (*SSB*) becomes the foundation for the valleys in the **Right** image. Consciousness is not separate from physics and matter in general, but is its highest ordered form.

Mapping to CA-SOM Energy

If mesoscopic neural variables emerge as the effective classical limit of microscopic quantum neurodynamics, the next question is whether their collective organization reproduces the attractor geometry proposed in the *CA-SOM* framework. Let an emergent classical order parameter y summarize θ-field averages within cortical columns. Assume the effective stationary distribution of y conditioned on sensory drive X has the Gibbsian form,

$$p(y|X) \propto \exp\left(-\frac{E_{eff}(y|X)}{T_{eff}}\right),$$

where y is a classic, coarse-average ordinal parameter per column (e.g. mean phases/activities), X external (sensory) stimulus/condition, E_{eff} effective energy including cooperativity, drive and input coupling. It collects contributions from *SSB* (favoring coherence), driving potentials (matching input), and interactions (couplings between local y's). This gives macroscopic statistics determined by the energy landscape. We assert a map $y \to s$ (Hopfield state) and $y \to m$ (slow feature code) such that

$$E_{eff}(y|X) \approx E_C[s(y), m(y)|x],$$

where $s(y)$ and $m(y)$ are smooth projections of effective variables y on Hopfield/*SOM* parameters with E_C the composite *CA-SOM* energy derived above and approximation gives equivalence in terms of dominant members and topology of minima. Quantum-classical coarsening produces the same type of energy landscape as *CA-SOM*. This asserts that, under decoherence and coarse-graining, the effective potential over classical variables reproduces the

CA-SOM energy landscape. The technical path consists of first integrating out fast quantum fluctuations σ to obtain effective action $S_{eff}(\theta_{low})$. We then introduce Langevin dynamics for θ_{low} with noise from environment to stationary Fokker–Planck equation. We define $y = G(\theta_{low})$ coarse-grained per column and assume weak-noise limit leading to most probable y minimizing E_{eff}. Finally, we identify E_{eff} minima with *CA-SOM* attractor minima, with topographic couplings K_{ij} inherited from spatial gradients of θ and short-range interactions, and mismatch terms from coupling to external drive X, paralleling the *SOM* energy terms. We start from Lagrangian $\mathcal{L}$ with the potential defined as

$$V(|\Phi|^2) = \lambda(|\Phi|^2 - \eta^2)^2,$$

and expand Φ around *SSB* minimum,

$$\Phi(x) = [\eta + \sigma(s)]exp\ i\theta(x).$$

To separate scales, we integrate out σ (massive part), retaining effective phase action

$$\theta_{massless} \to S_{eff}(\theta) \approx \int d^4x(\partial\theta)^2 + U_{ext}(\theta; X) + interaction,$$

$$\frac{dp}{dt} = \nabla_\theta \cdot \left(p\nabla_\theta E_{eff} + T_{eff}\nabla_\theta p\right),$$

where $(\partial\theta)^2$ penalizes fast changes (smoothness in space-time), U_{ext} is a weak drive from environment/input X. It encodes weak coupling to external drive X (sensory input), and spatial interaction penalizes rapid changes in θ. Adding environmental coupling to quantum Langevin for θ gives an open quantum system in the classical stochastic limit with δ-correlated ζ,

$$\frac{d\theta}{dt} = -\frac{\delta S_{eff}}{\delta\theta} + \zeta,$$

where $\frac{\delta S_{eff}}{\delta\theta}$ gives deterministic drift towards E_{eff} minima and ζ stochastic excitation (noise) of the environment. The associated Fokker–Planck equation gives description of the evolution of the distribution in the effective energy landscape,

where $p(\theta, t)$ is probability density, ∇_θ is the gradient in θ-space. The first term is a drift towards E_{eff} minima, the second gives diffusion through the forest. Stationary solution is

$$p^*(\theta) \propto \exp\left(-\frac{E_{eff}(\theta)}{T_{eff}}\right).$$

Coarse graining θ over a columnar patch Ω_i defines

$$y_i = \frac{1}{|\Omega_i|}\int \Omega_i\theta(x)dx,$$

where Ω_i denotes spatial i-th region, a cortical column in our case, $|\Omega_i|$ is the Lebesgue measure (volume) of the domain region of integration Ω_i. This averaging reduces the microscopic phases to the meso-equivalent y_i. Under mean-field approximations we have,

$$E_{eff}(y) \approx -\frac{1}{2}\sum_i\sum_j J_{ij}y_iy_j - \sum_i \beta_i(X)y_i + \lambda'\sum_i y_i^2\|X - m_i\|^2,$$

which identifies the Hopfield interaction part and *SOM* discrepancy, where J_{ij} is effective intercolumnar neurocoupling, short-range in neurotopology (related to K_{ij}), $\beta_i(X)$ are external biases that depend on the input X, $\lambda' > 0$ denotes weight of discrepancy with mapped prototypes. J_{ij} are shaped by spatial couplings decaying with distance (hence K_{ij}), and $\beta_i(X)$. Finaly, identifying y_i with s_i (binary or saturating continuous nonlinearity), we recover

$$E_C(s|x,m) = -\frac{1}{2}\boldsymbol{S}^T\boldsymbol{W}\boldsymbol{S} - \boldsymbol{b}^T\boldsymbol{S} + \lambda\sum_j s_j^2\left\|X - m_j\right\|^2 h_{ij},$$

demonstrating one route from quantum stochastic dynamics to the *CA-SOM* classical energy.

The Quantum Brain

These derivations clarify the possible role of quantum physics in consciousness without committing to strong quantum-computational interpretations of the brain. The above does not deny that quantum mechanics underwrites all chemistry, including synaptic release and ion channel gating. Rather, it demonstrates that coherent quantum superpositions at macroscopic neural scales are not needed and essential to explain conscious access. But again, this does not exclude quantum neurodynamics. Quantum-origin randomness contributes to neural noise and may influence neural variability and stochastic resonance in sensory detection (12, 74, 75). Hypotheses such as Hameroff-Penrose *Orch-OR* posit orchestrated tubulin-level coherence generating conscious moments (**Fig. 16**) (101, 102). However, decoherence analyses and lack of robust neurocoupling mechanisms to mesoscale dynamics cast doubt on this premise in brain neurophysiological conditions (31, 47, 48, 103). Conversely, electromagnetic field theories posit that the brain's classical *EM* field integrates information (97). Such fields are directly accounted for by classical Maxwell–Hodgkin–Huxley–mean-field dynamics and do not require quantum coherence (12, 104, 105). The framework here clarifies the role of physics: the macroscopic order parameter $C(t)$ emerges from classical, nonlinear, noisy neurodynamics

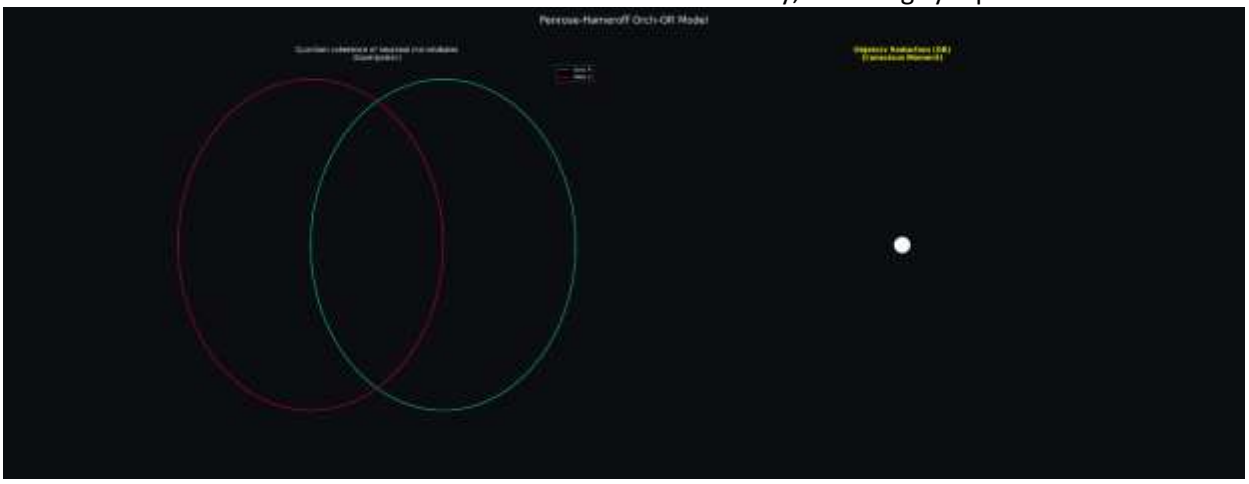


Fig. 16. Hameroff-Penrose Orch-OR Theory of Consciousness. Geometry of Consciousness: Consciousness is shown not as calculation (algorithm), but a physical event in the very geometry of space-time (splitting and merging states). **Brain Neuronal Microtubules:** The circles represent tubulin states. When they are too far apart (energy E_G becomes too great), the system bursts into reality causing collapse, objective classical supracritical reduction choosing the one of potential previously superposed state alternatives. **Neural Process (not state):** Consciousness according to this model is not something we have, but something that happens thousands of times per second (as a frequency).

constrained by neurostructural anatomy, brain neurohistology and metabolism. At the classical

level of consciousness, any quantum contributions thus appear as noise and parameter renormalizations that are already modeled in η- and σ_{eff}-terms.

Plausibility and Constraints

Taken together, these results suggest a formally consistent but empirically constrained route through which hypothetical microscopic quantum neuroprocesses could reduce to classical cortical consciousness neurodynamics. This derivation shows formal compatibility, not necessity, of a quantum substrate with the classical *CA-SOM* neurodynamics. It retains decoherence constraints (fast environmental coupling) and leverages stochastic quantization and *SSB* to produce an effective classical Gibbsian measure. Whether real cortical tissue supports the hypothesized coherent fields remains open and controversial (31, 47, 48, 66, 67). The value of the shown derivational method is to show that, if such a substrate really existed, the emergent classical neurodynamics naturally inherit: (i) an energy-based attractor geometry; (ii) short-range neurocouplings; (iii) input-dependent biases; and (iv) a two-timescale adaptation (fast state relaxations on a slow-changing metric), which are all consistent with *CA-SOM* and cortical neurophysiology.

Consciousness-to-Networks Downward Causation: Retrograde Neurofeedback of Consciousness onto Cortical Neural Networks and Self-Sustaining

Conceptual Role of Consciousness Retrograde Neurofeedback

If conscious access emerges from cortical attractor neurodynamics, an immediate question follows: can the resulting conscious state subsequently regulate the very neural substrate that generated it? We propose that consciousness acts not merely as an output of its generative neurodynamics, but as an active retrograde complex control neurosignal. Conscious access is not only the outcome of cortical neurodynamics. It also modulates subsequent processing with attention biasing relevant features. Global workspace ignition broadcasts selected content and predictive coding sends top-down predictions that shape lower-level responses (**Fig. 17**) (2, 9, 11, 28, 68-72). In *CA-SOM* model, retrograde neurofeedback implements a closed loop: once an attractor s^* is stabilized, it modifies neuroactivation thresholds, neural gains and neuroplasticity in both recurrent and neural map layers, thereby enhancing consistent neural inputs and suppressing distractors.

Formal Retrograde Neurofeedback Terms

To formalize this downward causal influence, we introduce explicit retrograde neurofeedback laws through which stabilized conscious attractors modify network neurodynamics, oscillatory neurocoherence, and neuroplasticity. Let $s^*(x)$ be the stabilized attractor for input x

given current m. We propose the following neurofeedback laws:

Retrograde Bias Neuromodulation in Hopfield Neural Layer. It is given by

$$b_i = b_i + \beta(Ws^*)_i + v[Va(x)]_i,$$

where V maps Kohonen *SOM* activation to recurrent biases β and v, s^* denotes stabilized attractor (current conscious content), $(Ws^*)_i$ reverberant self-amplification through existing neuroconnectivity and $Va(x)$ is projection of topographic activations in bias; V is the mapping matrix, $\beta, v \geq 0$ are neurofeedback strengths. b_i reinforces self-consistent

configurations and top-down alignment. This increases the alignment of local fields with the current global content (self-consistency amplification).

Neural Gain Neuromodulation via Oscillatory Neurocoherence. Coherent-phase synaptic neuromodulation is defined as

$$W_{ij}^{eff} \leftarrow W_{ij}\left[1 + \rho\cos\left(\phi_i - \phi_j\right)\right],$$

where ϕ_i represents oscillator phase of i-th unit, $\rho \geq 0$ is coherent gain amplitude with phases ϕ_i is entrained by s^*. Phase-aligned units get a higher effective coupling (communication through neurocoherence). Coherence among units participating in s^* increases their mutual neural coupling (41, 42, 44).

Kohonen *SOM* Neuroplasticity Gating. Attentional learning/attention-controlled neuroplasticity is given by

$\alpha_{eff}(s^*) = \alpha_0[1 + \gamma A(s^*)]$, with $0 \leq A(s^*) \leq 1$,

where α_0 is a base learning rate, $\gamma \geq 0$ is the coefficient of amplification by attention/stability of content, $A(s^*)$ is an attention scalar measure of attractor stability/energy gap (e.g. $\Delta E = E_C - E_C(s^*)$, where E_C denotes the nearest competitor). Consciously accessed content accelerates the consolidation of relevant codes. Update rule is then

$$m_j = m_j + \alpha_{eff}(s^*)h_{ij}\left(x - m_j\right).$$

Thus, when a robust content is accessed, *SOM* feature codes supporting it are preferentially consolidated (36, 39, 86).

Neighborhood Radius Adaptive Neuromodulation. It is described as

$$\sigma(s_t^*) \leftarrow \sigma_0[1 + \kappa B(s^*)],$$

where σ_0 is basic neighborhood width, $\kappa \geq 0$ is modulation strength, $B(s^*)$ is novelty/uncertainty measure. It increases for

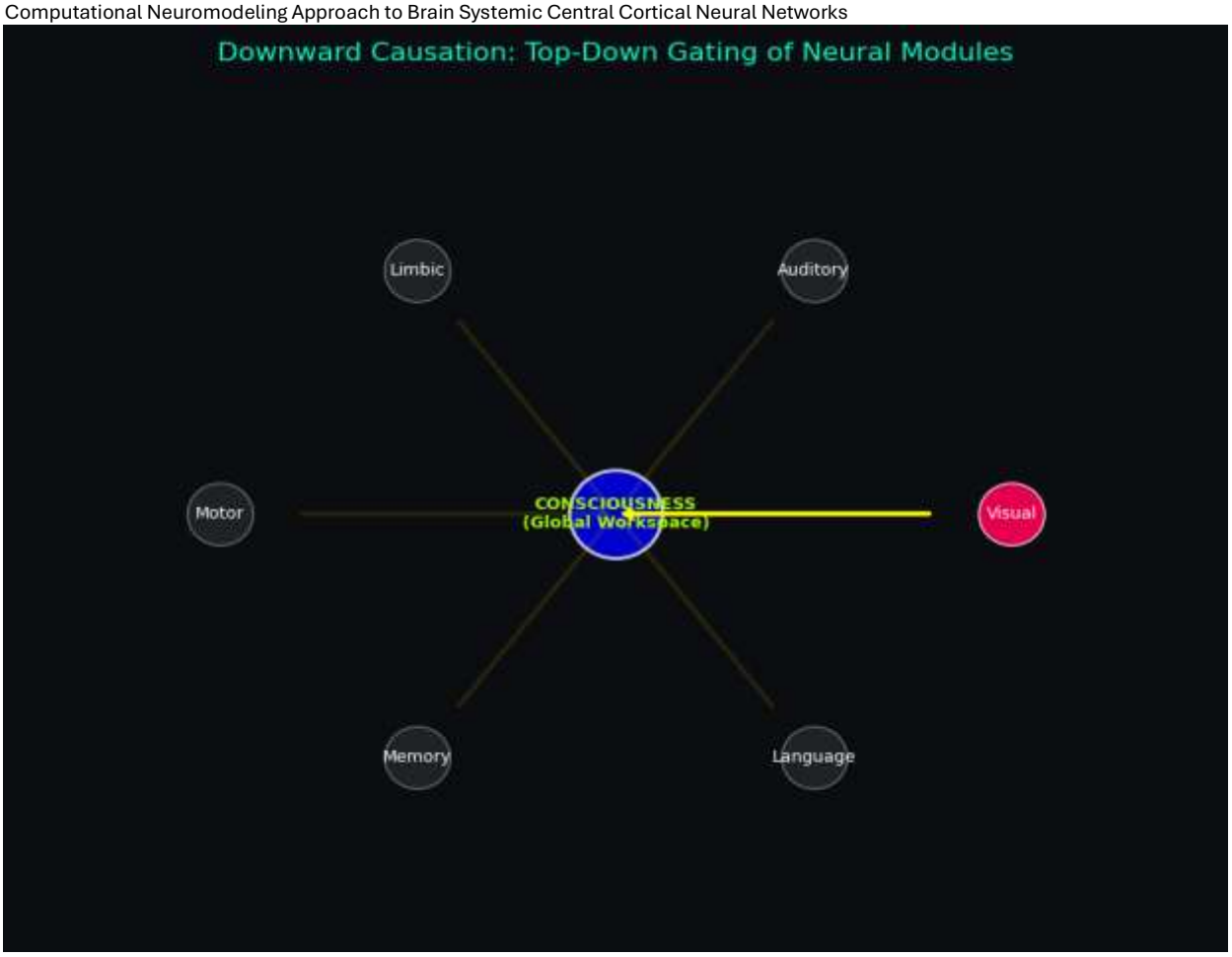


Fig. 17. Retrograde Consciousness-Induced Top-Down Gating of Neuromodules. Here the consciousness chooses which Baars-Franklin's neuromodule (e.g. vision, hearing, emotions) will be illuminated by attention. Consciousness acts as a reflector that enhances the activity of one neuromodule, while keeping the others in the shadows. The central circuit (Global Central Neural Workspace) sends strong neurofeedback arrows to the small peripheral circuits (neuromodules), selectively igniting them, i.e. it represents active Baars-Franklin's Neuromodule Selector.

novel or high-uncertainty contents, widening the neighborhood to promote exploration. It expands the neighborhood when it is new, narrows it when it is familiar. For familiar contents, σ narrows to refine representations. This gives neurodynamic balance between exploration and exploitation in neural mapping.

Control Law: $C(t)$ Modulates Multiplicative Gain, Neural Coupling and Neurosynchrony

While the previous neurofeedback terms describe local mechanisms, a more global formulation is needed to explain how the emergent conscious state regulates cortical neurodynamics at the systems level. We

therefore introduce a control law governed by the order parameter of consciousness $C(t)$. We now formalize how the emergent order parameter $C(t)$ feeds back to regulate its own substrate, i.e. how retrograde neurofeedback

changes effective nonlinearities and neural coupling. Consider the mean-field cortical neurodynamics

$$\frac{dx}{dt} = F(I_{ext} + \eta + xW) - x,$$

with gains and couplings depending on C. We define the following neurodynamical parameters:

Gain neuromodulation,

$$g(C) = g_0(1 + \beta_C C),$$

Neurocoupling modulation,

$$W(C) = W_0 + \Delta W_C C,$$

and thalamocortical neurosynchrony modulation in the Kuramoto neural coupling,

$$K(C) = K_0 + \kappa_C C.$$

The controlled neurodynamics are then given by

$$\frac{dx}{dt} = \eta - x + \phi\big[g(C)\big(I_{ext} + xW(C)\big) - \theta\big],$$

where $g(C)$ is gain modulated by the ordinal parameter of consciousness C, $W(C)$ is neuroconnectivity modulated by C, η is excitation/synaptic noise. Linearizing around a working point x^*, the Jacobian becomes

$$J(C) = g(C)D_\phi(x^*)W(C) - I$$

The derivative of the leading eigenvalue λ_{max} with respect to C is approximately given by

$$\frac{d\lambda_{max}}{dC} \approx D_\phi(x^*)(g_0 v^T \Delta W_C u + \beta_C g_0 v^T W_0 u),$$

where u and v are the right and left eigenvectors of the critical mode associated with λ_{max} at $C = 0$ and $D_\phi(x^*)$ is a local slope of nonlinearity. Positive derivative of λ_{max} over C indicates that increases in C further increase the net gain of the critical mode, providing a mechanism for ignition stabilization and hysteresis. However, stability requires that, beyond a certain C, homeostatic mechanisms curb growth with saturation for safety. One can implement a saturating $\beta_C C$ or subtractive adaptation to ensure boundedness.

Thalamic Retrograde Neural Loop

Because large-scale conscious access requires coordinated interareal communication, retrograde control must also involve subcortical mechanisms responsible for neurosynchronization and routing. The thalamus provides a neurobiologically plausible substrate for such global neural system coordination. The thalamus mediates global neurosynchronization at consciousness access. Its nuclei, notably pulvinar and mediodorsal nuclei, coordinate cortical interneural communication through neurocoherence and gain control (18, 23, 106). We model a thalamic gain variable g_{th} that increases effective coupling (K) and coherence with C-dependent input as

$$\tau_{th}\frac{dg_{th}}{dt} = g_{th,0} - g_{th} + \delta_C C(t),$$

where δ_C quantifies the strength of the retrograde neurofeedback influence of consciousness on the thalamus. Thalamic gain increases $K(C)$ in the Kuramoto neurodynamics and selectively enhances neurocoupling among task-relevant areas, consistent with attention-dependent routing (18, 23). This closes a rapid retrograde loop: ignition raises C, which increases thalamic gain and interareal neurosynchrony, further stabilizing the conscious state, thus closing the neuroreverberant circle.

Neuromodulatory Implementation and Behavioral Correlates

Beyond thalamic neurosynchronization, conscious stabilization is likely supported by diffuse neuromodulatory systems that neurodynamically regulate neural gain, arousal, and precision weighting across cortical networks. Biophysically, C-dependent gain control can be implemented via neuromodulators. Norepinephrine from locus coeruleus (*LC-NE*) increases gain and promotes network integration under uncertainty, correlating with pupil dilation and pupilometric

P_3 amplitude (24, 29, 78). Acetylcholine modulates sensory precision and thalamocortical gating (17, 18). Dopamine broadcasts reward prediction errors and can serve as a global teaching signal (27, 30). We formalize a dynamical neuromodulatory gating variable $m(t)$ linking C to arousal neurophysiology and P_3/pupilometry obeying

$$\tau_m \frac{dm}{dt} = m_0 - m + \gamma_C C(t) + \gamma_{PE} PE(t),$$

where $PE(t)$ is a prediction error or surprise signal, and m as global neuromodulatory gain variable (e.g. *LC-NE*) modulates $g(C)$ and $K(C)$, m_0 is the base value, γ_C and γ_{PE} are coefficients of influence of awareness and surprise/error. This captures arousal-linked enhancement of conscious access and retrograde stabilization.

Retrograde Control Predictive Coding

If consciousness exerts top-down regulation, this influence should also shape predictive inference by neuromodulating the balance between internally stabilized content and incoming prediction error. In the predictive coding formulation, let $E(t)$ be total error energy. We define a composite control neurosignal,

$$U(t) = aC(t) - bE(t),$$

and set gain and neurocoupling modulation proportional to U:

$$g(C, E) = g_0(1 + \beta_U U),$$

where a and b are weights for order parameter and error energy, respectively, β_U is gain sensitivity to the control neurosignal. This represents a closed loop that favors stable, consistent content and discourages inconsistent one, i.e.

$$W = W_0 + \Delta W_U U.$$

This implements an adaptive neurocontroller that functions in the following manner: when conscious access increases and errors decrease, U rises, strengthening the pathways supporting the accessed content and vice versa, when errors rise, U falls, reducing gain and encouraging exploration or switching. The neurocontroller can be tuned to maintain the system near a critical regime of high neurodynamic range and sensitivity (15, 17, 25, 45, 80, 81, 107).

Three-Factor Learning Rule with C as a Global Factor

A persistent retrograde influence should not only regulate ongoing neuroprocessing, but also bias future network organization through learning and neuroplasticity. To formalize how conscious access shapes neuroplasticity, we posit an objective function J that rewards global availability and internal consistency while penalizing metabolic cost, i.e.,

$$J = \lambda_1 I(S; C) + \lambda_2 \Phi(x) - \lambda_3 E_{metab.},$$

where $I(S; C)$ is mutual information between stimulus S and order parameter C, $\Phi(x)$ is a surrogate for integration (e.g., a network-level approximation to *IIT*'s Φ), and $E_{metab.}$ reflects average firing and neurosynaptic activity (5, 82). Synaptic weights w_{ij} are updated via gradient ascent,

$$\frac{dw_{ij}}{dt} \propto \frac{dJ}{dw_{ij}}$$

Under tractable approximations, this yields a three-factor rule:

$$\frac{dw_{ij}}{dt} = \eta \, pre_i post_j M(t) - \alpha w_{ij}$$

where $M(t)$ is a global neuromodulatory factor proportional to $C(t)$ (and potentially to dopamine/*NE*), pre_i and $post_j$ are pre- and postsynaptic activities, and α enforces weight decay (26, 27). This aligns with known neuromodulated spike-timing-dependent neuroplasticity and provides a credit-assignment signal tied to access: when content is consciously accessed (high C), synapses supporting it are strengthened, biasing future neuroprocessing.

Energy Tilt and Convergence

The cumulative effect of retrograde neuromodulation is expected to reshape the effective attractor landscape itself (**Figs. 18**, **19**), stabilizing consciously accessed states against perturbation. We define

$$E_C^{fb}(\boldsymbol{s}) = E_C(\boldsymbol{s}) - \varepsilon \mathbf{s}^T \mathbf{W} \boldsymbol{s}^* - \varepsilon' \mathbf{s}^T Va(x),$$

where $\varepsilon, \varepsilon' \geq 0$ are return slope coefficients capturing neurofeedback strength, $\mathbf{s}^T \mathbf{W} \boldsymbol{s}^*$ is projection of the candidate $\mathbf{s}$ onto the axis of the current content $\boldsymbol{s}^*$ and $\mathbf{s}^T Va(x)$ is alignment with neurotopographical excitation. It increases the pool volumes around $\boldsymbol{s}^*$ and accelerates reattraction, i.e. the gradient of E_C^{fb} at $\boldsymbol{s}^*$ gains negative curvature along directions aligned with $\boldsymbol{s}^*$, increasing local basin volume and speeding reattraction after perturbations (Hessian matrix under feedback),

$$\frac{d^2}{ds_j ds_i} E_C^{fb}(s) = \frac{d^2}{ds_j ds_i} E_C(s) - \varepsilon W_{ij},$$

where the second derivative (Hessian) determines the local curvature (stability). Subtracting εW_{ij} softens the curvature along lines aligned with $\boldsymbol{s}^*$ (wider basin). It gives controlled neuromodulation of stability without violating the boundedness from below. If $\boldsymbol{W}$ is positive-semidefinite on the subspace

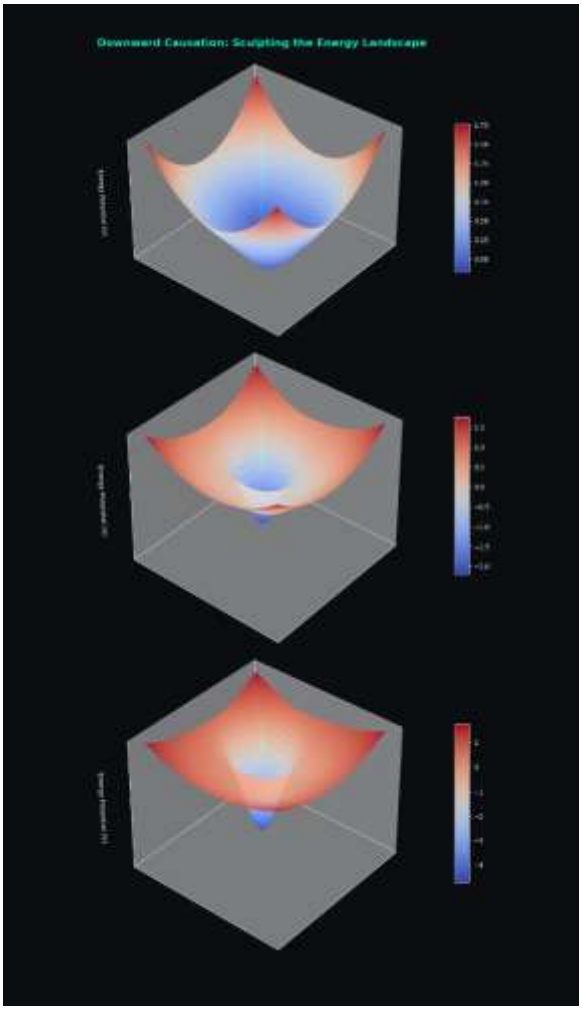


Fig. 18. Retrograde Consciousness-Induced Sculpting of a Cortical Attractor Landscape. Neural Process of Thought Stabilization: Without consciousness (small value of consciousness attention parameter in the model – measure of consciousness-to-networks downward causation strength), thought would easily leak into the noise. With a high value of attentional strength, consciousness makes a stable pool of attraction (from **Top to Down** the respective values of conscious attentional strength parameter are *A* = 0.3, *A* = 2.5, and *A* = 5.0). It explains how we keep focus on complex problems. **Real-Time Neuroplasticity:** This is not just learning (long-term memory), but an instantaneous change in cortical network

neurodynamics under the influence of a global conscious state. **Force vector:** The arrow represents a consciousness-induced mental pressure that changes the probability of physical states of network neurons with consequential deepening of the attractor stabilizing it that way.

associated with $\boldsymbol{s}^*$, the Hessian becomes more positive at competitor states and more negative along the $\boldsymbol{s}^*$ directions, which increases basin dominance without destroying Lyapunov descent (provided $\varepsilon < \varepsilon_{max}$ ensuring E_C^{fb} remains bounded below).

Stability Conditions, Robustness and Energy Costs

However, any self-reinforcing neurofeedback architecture must satisfy neurodynamical stability constraints to avoid pathological runaway excitation or oscillatory instability.

Fast Neural Loop. For fixed m, b, W_{eff}, asynchronous flips maintain $E_C^{fb} \leq 0$. If ε and ρ are small enough that W_{eff} remains symmetric and $\|W_{eff}\|$ bounded, convergence is preserved (38).

Slow Neural Loop. Kohonen *SOM* learning with $\alpha_{eff}(\boldsymbol{s}^*)$ obeying Robbins–Monro still converges (39, 86) for bounded α_{eff} if $E[A(\boldsymbol{s}^*)]$ is bounded and applies

$$\sum \alpha_{eff} = \infty,$$

$$\sum \alpha_{eff}^2 < \infty.$$

Neurooscillatory Coupling. If phase neurodynamics are slaved to $\boldsymbol{s}^*$ (e.g., $\phi_i = \Phi(s*)$), then W_{eff} remains time-periodic. Averaging theory shows convergence to a time-averaged Lyapunov function if neurooscillation is fast compared to flipping neurodynamics; or, practically, synchronous regimes effectively enhance neurocouplings during the up cycles (42, 44). Stability analysis requires that the closed-loop neural system avoids runaway excitation and neurooscillations. Thus, avoiding divergence maintains the work regime within neurophysiological limits. If the open-loop Jacobian J_0 has largest eigenvalue $\lambda_0 < 0$, and neurofeedback adds eigenvalue nonlinear stability (a saturating positive neurofeedback),

$$\delta\lambda(C) = k_1 C - k_2 C^2,$$

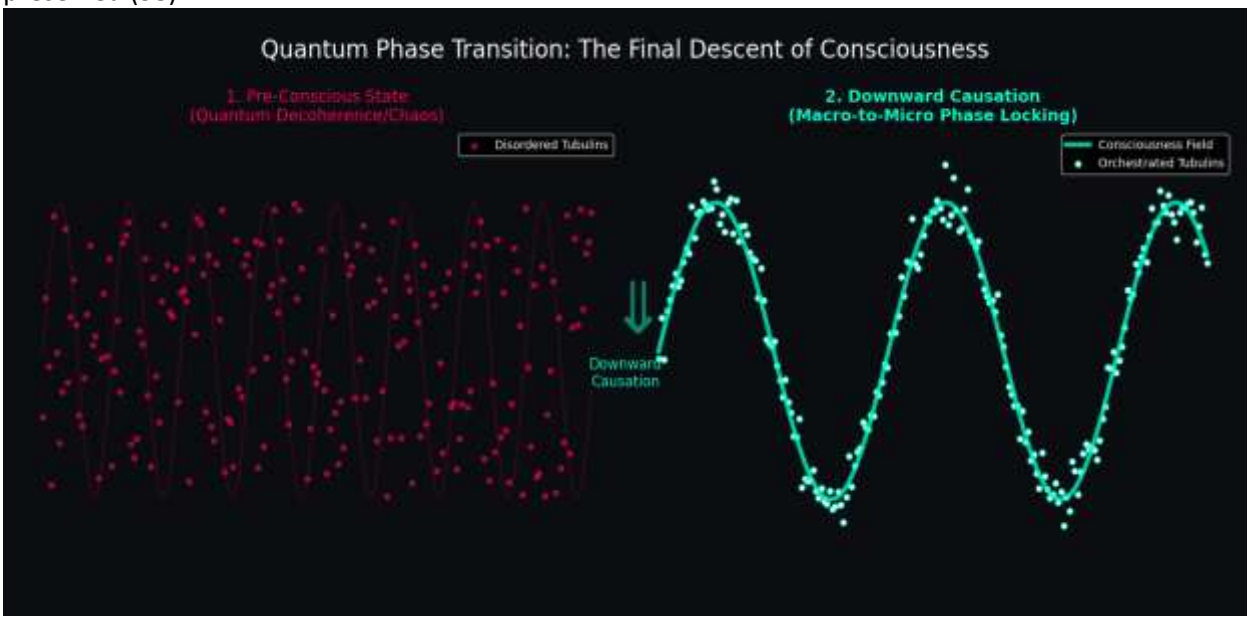


Fig. 19. Downward Causation of Neuroquantum Consciousness. Phase-Locking: (Left) Disordered and chaotic tubulins of brain neuromicrotubules. **(Right)** The tubulins (white dots) are no longer moving, but follow the path of a big wave of consciousness. That's how macro-state controls micro-neurophysiology. **Neuroquantum Reduction (Hamerrof-Penrose *Orch-OR*):** This visually explains Hamerrof-Penrose *Orch-OR* Theory that consciousness is not a calculation, but a specific physical event that brings order to the structure of space-time within neurons. **Causal Primacy of Consciousness:** This shows that consciousness has the last word, i.e. it chooses the final outcome of neuroquantum processes, which also solves the problem of free will, by the way.

where $k_1 > 0$ is positive neurofeedback at low C (ignition stabilization) and $k_2 > 0$ is saturation negative neurofeedback at large C (safe limit), then the net eigenvalue is

$$\lambda(C) = \lambda_0 + \delta\lambda(C).$$

Stability requires $\lambda(C) < \lambda_{safety}$ for all admissible C, enforced by $k_2 > 0$ and ceiling on C from metabolic constraints (λ_3 term in J) (82). Energy costs constrain sustainable firing rates and neurosynchronization, enforcing a narrow viable range for ignition, consistent with the fragility of conscious access under sedation and sleep (4, 82). This analysis predicts a characteristic hysteresis loop in C as a function of input strength and neuromodulatory state, testable via *TMS-EEG* and pupil-linked arousal manipulations (73, 78).

Relation to Neural Global Workspace and Predictive Coding

Having formalized the retrograde mechanisms, we now examine their conceptual compatibility

with dominant cognitive theories of consciousness.

Ignition. b_i and W_{eff} neuromodulation implement a global neuroamplification consistent with *GNWT* ignition: a selected content gains widespread, self-sustaining activation (2, 9).

Predictive Coding. Top-down bias terms ($b \sim$ predictions) reduce mismatch at lower levels, equivalent to reducing E_{SOM} in regions consistent with $\boldsymbol{s}^*$, while increasing mismatch elsewhere, biasing the next input-dependent attractor (11, 28, 68-72). Thus, retrograde feedback aligns map codes and attractor states across layers and scales, supporting neurocoherent serial episodes of conscious content.

Testable Predictions and Predicted Observable Signatures

A theory of consciousness gains explanatory value only insofar as it generates empirically testable predictions. The proposed retrograde neurofeedback framework therefore implies several observable neurophysiological signatures.

Disrupted Neurotopography. Some studies have demonstrated difficulty forming coherent attractors for complex stimuli despite intact local features, so-called fragmentation of experience, shown in the case of focal lesions in *SOM*-like areas (32, 34, 87, 88).

Disrupted Neurorecurrence. In this case, it is expected mental content instability, shortened dwell times, and reduced ignition probability. This is all shown in the case of pharmacological *NMDAR* hypofunction (6, 11, 68, 69).

Enhanced/Disrupted Oscillatory Neurosynchrony. It is expected that synchronous neurodynamics should modulate attractor basin depth and access probability. Also, gamma-phase alignment predicts better binding and faster recognition (6, 41, 42, 44, 69).

Cross-Frequency Signature. During conscious access, alpha/beta neurofeedback phase modulates gamma amplitude more strongly and more globally, increasing R_{γ} and $R_{\alpha\beta}$ neurocoherence. Disruption of deep-layer neurofeedback (e.g., by laminar-specific *TMS*) reduces C selectively (14, 22, 25). **Ignition Threshold Shift.** Increasing arousal (pupil) lowers the input threshold for ignition and increases hysteresis. Neuropharmacologic *NE* blockade raises threshold and reduces hysteresis (24, 29, 78). ***PCI* Dependence.** The perturbational complexity index rises when the system is held near but below the ignition threshold (high metastability) and falls during deep unconsciousness. During strong, sustained ignition it remains high but more structured, with reduced diversity of evoked patterns (45, 73). **Credit Assignment.** Stimuli that reach conscious access produce larger, longer-lasting neurosynaptic changes in associated pathways than subthreshold stimuli, measurable via changes in effective neuroconnectivity (26, 27).

Discussion

This study offers a neurocomputationally explicit account of how classical brain network processes generate consciousness, how any plausible neuroquantum contributions reduce to classical limits at neural scales, and how the emergent macroscopic order parameter $C(t)$ retroacts onto cortical networks to stabilize and shape consciousness neuroprocessing. We developed a *CA-SOM* computational neuromodel that unifies neurotopographic organization and attractor neurodynamics within explicit neocortical constraints. Together, the derivations and models integrate neurostructure, neurophysiology, neurodynamics, and neurophysics into a coherent central neural process where conscious access is an emergent, metastable regime of global integration supported by cortical laminar predictive coding, thalamocortical neurosynchronization, and neuromodulatory gain control (2, 4, 11, 12, 14, 16-23, 25, 40). Provided the energy-based convergence and multi-timescale stability of the model, we propose information-theoretic alignment of neural maps and attractors, embedding oscillatory neuromodulation consistent with neural communication-through-neurocoherence. We further show how such classical neurodynamics can arise as a limit of a quantum field substrate under quantum decoherence and stochastic quantization, leading to an effective Gibbsian energy that maps naturally onto *CA-SOM* neuromodel. Finally, we formalize retrograde neurofeedback as a set of neuromodulatory terms that tilt the energy landscape, gate neuroplasticity, and shape oscillatory neurocoupling, reconciling the model with *GNWT* ignition and predictive coding.

Novelty Neuroscientific Contributions of the Model

Our *CA-SOM* computational neuromodel of consciousness gives a few novel insights into the structure and function of the consciousness system. The model proposes a multiscale mechanism by which distributed cortical representations are transformed into metastable, globally accessible cortical attractor states through the interaction of neurotopographic organization, associative neurodynamics, predictive neuromodulation, and cross-scale neurooscillatory coordination. Here, Kohonen *SOM* determines slowly adapting neurotopographically organized cortical representations, Hopfield neural layer turns these representations into fast stabilizing cortical attractor neurodynamics, predictive coding modulates cortical attractor landscapes, oscillatory neural gating/coupling coordinates

these events, *GNW* enables global accessibility, while consequent, generated integrated metastable network state represents consciousness. Therefore, according to our model of consciousness, conscious access emerges when a neurotopographically constrained cortical representation crosses an oscillation-dependent attractor-stabilization threshold, producing a metastable globally integrated cortical network state that subsequently feeds back to reshape the underlying cortical energy landscape. Here, microscopic quantum neurodynamics provide a hypothesized substrate whose coarse-grained effective neurodynamics enter the classical *CA-SOM* neurodynamic model. The quantum layer is therefore treated as a formally derived substrate constraint rather than as an empirically established mechanism of consciousness processing. We can say that *CA-SOM* contribution, in general, is contained in a single multiscale neurodynamical mechanism linking representation, attractor stabilization, neurooscillatory gating, global access and retroactive neural network neuromodulation. We offer and specify the specific, multiscale neurodynamical coupling framework that connects these levels of consciousness functioning with specific mapping of each of these particular levels in this global framework. This is summarized in **Table 1** and **Fig 20**. Additionally, our integrative model generates a set of experimentally discriminable, falsifiable and testable predictions (**Table 2**).

Neurobiological Plausibility of the Model

In our model, cortical columnar organization and laminar neural circuits are modeled explicitly, i.e. map units correspond to cortical columns, while recurrent Hopfield cores represent local and interareal neural loops (11, 16, 19, 32-34), thus providing deeply rooted starting logical premises of the model. Here, oscillatory neurodynamics plays central role to effective neural connectivity. Our model predicts distinct frequency channels for neural feedforward/feedback connections as also shown empirically (6, 41-44). Multi-timescale neurodynamics match observed cortical hierarchies with distinct intrinsic timescales (108), mapping onto slow neural map adaptation and fast mental content stabilization.

Relation to Existing Theories of Consciousness

The framework combines key insights from *GNWT* and recurrent neuroprocessing theories. Retrograde neurofeedback and neurooscillatory gain implement ignition and global broadcasting; convergence to a dominant attractor captures all-or-none conscious access (2, 4, 9, 69). The ignition phenomenon and global broadcasting captured by $C(t)$ echo *GNW's* emphasis on fronto-parietal recruitment and a late, non-linear access threshold (2, 4, 46). Simultaneously, the reliance on recurrent neuroconnectivity, cortical translaminar neurofeedback, and rapid, content-specific neural loops aligns with recurrent neuroprocessing accounts (8). By formalizing band-limited interactions (gamma and alpha/beta neurofeedforward), we incorporate a mechanistic instantiation of predictive coding microcircuits for conscious access that has been documented across multiple levels of the visual hierarchy (11, 22). The top-down bias terms and mismatch-driven *SOM* updates formalize prediction and prediction-error minimization within the same energy landscape (11, 28, 68-72). Furthermore, defining $C(t)$ as a product of neuroactivation and neurosynchrony subject to

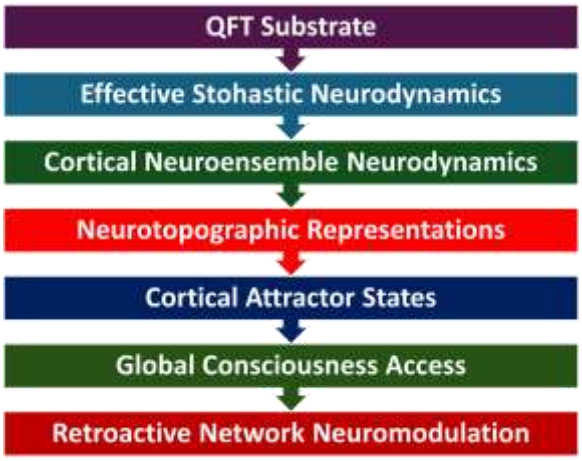


Fig. 20. Multiscale Causal Architecture of the CA-SOM Model of Consciousness

an error-based criterion helps bridge the integration–differentiation tension emphasized by *IIT*. *CA-SOM* embodies integration through attractor unity (Hopfield) and composition through neuromap structure (*SOM*). Content reaches consciousness when widespread neurointegration is achieved without sacrificing internal consistency or differentiation (5, 73). The mutual information $I(H;S)$ increases as training proceeds, serving as a proxy for neurointegration under physical constraints (5, 10). Unlike exact Φ, which is intractable for large systems (5), $I(H;S)$ is computable and operationally meaningful. Yet it does not claim identity with experience, only correspondence with the neurointegrative structure. We employ Φ only as a conceptual guide for an integration surrogate. We did not adopt *IIT's* axioms, but our energy and neurosynchrony constraints are consistent with measurable increases in perturbational complexity during consciousness (73).

Cortical Neuromicrocircuit and Translaminar Neural Mechanisms

A central virtue of the proposed neuromodel framework is that it honors canonical neurocitoarchitectonic features. Repeating neural microcircuits with layer-specific inputs and outputs are not incidental. They are necessary for the spectral multiplexing of feedforward and neurofeedback streams, for the implementation of predictive coding, and for neuroapical dendritic amplification (11, 12, 14, 16, 19-22, 25). This explains why disrupting deep-layer neurofeedback or apical neurointegration impairs consciousness in anesthesia and brain lesions, and why selective thalamic lesions degrade global availability even when local activity persists (4, 18, 20, 23). The eigenvalue crossing analysis reveals how cortical laminar gain neuromodulation via neuroapical amplification (parameter β) acts as a proximate control knob for ignition: subtle shifts in deep-layer drive can push the network across the threshold, producing the hallmark nonlinearity in access (20, 46).

Thalamic Spectral-Temporal Neurodynamics

By embedding the mean-field rate neurodynamics within a Kuramoto neurosynchronization framework, we formalized how thalamus and cortico-cortical neurocouplings implement communication-through-neurocoherence (18, 22, 23). The order parameter $R_\gamma \times R_{\alpha\beta}$ reflects the neurocoupling of bottom-up evidence with top-down hypotheses. Consciousness access requires both to exceed critical values. The pulvinar's role in routing, adjusting effective K, explains attentional gating of access and the empirically observed band-specific neurocoherence patterns (18, 22, 23). This spectral logic predicts that alpha/beta neurofeedback should strengthen and shift the phase of gamma bursts in targets during consciousness access, whereas in unconscious states alpha/beta neurofeedback loses its organizing role, consistent with observations in anesthesia and sleep (4, 22, 25).

Quantum-to-Classical Reconciliation

We addressed a lingering conceptual tension in the literature about this matter: whether consciousness requires fundamentally quantum mechanisms. Our reduction from Lindblad dynamics to classical Langevin equations demonstrates that any quantum coherence at sub-neural scales is rapidly destroyed by environmental interactions, leaving classical,

Table 1. Conceptual advance of the *CA-SOM* framework

Existing framework	General	*CA-SOM*
Kohonen *SOM*	Neurotopographic organization	Links neurotopography to cortical attractor stabilization
Hopfield layer	Associative cortical attractors	Embeds attractors in cortical neurotopography
Predictive coding	Prediction/error minimization	Incorporates prediction into same energy landscape
GNW	Global access/ignition	Gives ignition an explicit attractor transition
Neurooscillatory behaviour	Communication/synchronization	makes synchrony a control Attractor accessibility parameter
***IIT*-based neurointegration**	Integration/differentiation	Provides computable structural proxy
Microscale neuroquantum level	Microscopic substrate	Derives a classical effective limit

noisy dynamics at the neural and mesoscopic levels (13, 31, 47, 48). Within this view, quantum consciousness is best understood as contributing stochasticity and parameter renormalizations already encapsulated in the noise terms of neural equations. This does not imply that quantum physics is irrelevant, it certainly remains the bedrock of molecular processes, but it does imply that macroscopic coherence or collapse-type events need not be invoked to explain consciousness. This position is consistent with decoherence estimates, with the rich success of classical neural modeling, and with the absence of reproducible evidence for long-lived, macroscopically significant brain quantum neurocoherence (31, 47, 48, 103). Proposals for nuclear spin-based processing offer interesting future avenues for probing subtle quantum-biological effects, but their linkage to fast, energy-intensive cortical neurodynamics still remains speculative and likely indirect (66).

Retrograde Neurofeedback and Learning

A crucial element of the account is consciousness retroaction upon its neurogenerator, i.e. once access emerges, it shapes its own future probability. We formalized this as *C*-dependent neuromodulation of gains, neurocouplings, and neuroplasticity. This retrograde loop explains several empirical phenomena. First, sustained consciousness despite brief occlusions or distractions reflects hysteresis due to *C*-dependent positive neurofeedback (gains and thalamic neurocoupling), a form of balanced neuroamplification across distributed areas (83). Second, arousal's facilitation of consciousness indexed by pupil dilation and *P3* amplitude arises from neuromodulator-mediated gain

increases that lower ignition thresholds (24, 29, 78). Third, the privileged role of conscious content in learning follows from three-factor neuroplasticity: when a representation reaches consciousness, a global neuromodulatory signal coincident with pre- and postsynaptic activity performs credit assignment, consolidating the contributing synapses (26, 27). This formalizes a functional advantage for consciousness: it is not strictly necessary for rapid perception, but it confers an enduring adaptive benefit by selectively stabilizing behaviorally relevant representations.

Testable Predictions

The framework invites multiple, falsifiable predictions (**Table 2**):

Table 2. Experimentally testable predictions of the Model

Neural function	Corresponding measurable observable correlate
Shorter cortical attractor dwell times	Disruption of neural recurrence
Altered cortical attractor basin depth	Altered neural synchrony
Consciousness access gamma cross-frequency coupling	Alpha/beta cortical rhythms
Cortical arousal	Ignition threshold shift
Ignition threshold	*PCI* dependence
Consciousness access	Enhanced neurosynaptic consolidation

Cortical Laminar-Specific Perturbation. Deep-layer targeted disruption (e.g., laminar *TMS* or optogenetics in animal models) should reduce *C* by attenuating neuroapical amplification and alpha/beta feneuroedback, even if superficial gamma feedforward remains intact. This should increase ignition thresholds and reduce *P3b* (4, 20, 22, 46).

Thalamic Gain Manipulation. Pulvinar stimulation should increase interareal neurocoherence (higher *K*), reduce the variance of ignition thresholds across trials, and increase reportability. Its inhibition should do the opposite (18, 23).

Neuromodulatory Levers. Neuropharmacologic manipulation of noradrenergic tone should shift thresholds and hysteresis widths, with concomitant changes in pupil-linked arousal and *P3* amplitude (24, 29, 78).

***PCI* State Dependence.** Bringing the system near the critical ignition threshold (via stimulation or neuromodulation) should maximize *PCI*, while pushing it into either subcritical (deep unconscious) or overly supercritical (seizure-like) regimes should reduce *PCI's* complexity profile (45, 73).

Neuroplasticity Tails. Trials that cross conscious access threshold (high *C*) should leave larger, longer-lasting traces in effective connectivity than near-threshold misses, detectable with pre/post neuroconnectivity estimation (26, 27).

Implications for Consciousness Disorders and Anesthesia

Clinically, the model reframes disorders of consciousness as disruptions to one or more components of the ignition loop: (i) loss of deep-layer neurofeedback and neuroapical amplification, (ii) impaired thalamic gain control and neurosynchronization, (iii) reduced neuromodulatory gain or (iv) structural damage to frontoparietal hubs. Anesthesia agents that preferentially target deep-layer pyramidal neurons or thalamocortical neurosynchrony should raise ignition thresholds and suppress alpha/beta neurofeedback, consistent with observed shifts in spectral power and neuroconnectivity under anesthesia (4, 18, 22,

23). The model thus motivates interventions that target specific deficits, e.g., thalamic stimulation to restore *K*, cholinergic augmentation to increase g, or patterned stimulation that re-establishes cross-frequency neurocoupling while monitoring *C*-linked biomarkers (*P3*, *PCI*, pupil).

Consciousness-Based Neural Engineering and Computational Neuroscience

For neuromorphic and brain–computer interface applications, the control law derived here suggests strategies for closed-loop neuroaugmentation of consciousness: (i) estimation $C(t)$ from multichannel recordings, (ii) gain neuromodulation and neurocoupling through neurostimulation or neuropharmacology to bias ignition and (iii) coupling learning to access via *C*-linked reinforcement. At the algorithmic level, the three-factor rule with *C* as a global factor suggests biologically plausible credit assignment approximations to backpropagation, where consciousness acts as a supervisor enhancing learning of globally useful features (26, 27).

Limitations of the Model and Opened Issues

Several limitations of our consciousness neural model warrant caution and that's because though our model looks conceptually plausible, some issues still need to be addressed here. First, mean-field reductions gloss over heterogeneity, nonlinear dendritic computations and non-Poissonian spike statistics. While the neuroapical amplification term partially addresses dendritic effects, more detailed multi-compartment neuromodels could refine the micro-to-macro neural mapping (12, 20, 21). Second, the Kuramoto neurosynchronization model abstracts away amplitude neurodynamics and complex cross-frequency couplings. Future work could adopt Wilson–Cowan neurooscillators or neural mass models that explicitly capture amplitude–phase interactions (12, 15, 25). Third is energy function for exact SOM learning, namely, the classical Kohonen rule lacks a global energy. We used a mismatch surrogate to couple to Hopfield energies and invoked stochastic approximation for convergence (36, 39, 86). This is a principled approximation rather than an exact Lyapunov derivation. The fourth is capacity and scaling. While modern Hopfield variants scale favorably (89, 90), biological constraints (sparseness, noise, synaptic limitations) will modulate effective capacity; parameter regimes need calibration. The fifth issue of our model is measuring integration. Our surrogate for integration Φ remains heuristic. Aligning the order parameter $C(t)$ with tractable, empirically validated complexity measures like *PCI* is a pragmatic step, but translating between different measures of integration and differentiation remains an open challenge (5, 73). $I(H;S)$ is only a proxy and connecting it to empirical markers of conscious level/content (e.g., *PCI*, perturbational complexity) still remains to be done. Sixth, the quantum-classical reduction presumes Markovian baths and weak nonlinearity in the Wigner calculus. Exotic regimes could, in principle, produce longer-lived neurocoherence, though the burden of proof is high to show macroscale functional relevance at physiological temperatures (13, 31, 47, 48, 66, 103). Our quantum-to-classical derivation is formal and agnostic about biophysical substrates (e.g., neuromicrotubules). Neural quantum decoherence at neurophysiological conditions is rapid (31), making sustained large-scale quantum coherence unlikely; the contribution here is a theoretical and computational pathway from *SSB* and stochastic quantization to *CA-SOM*-like energies, not an empirical claim of quantum computation in the brain (31, 47, 48, 66, 67). But if such computation exists then

this presents very probable and important neuroquantum mechanism of consciousness (100, 109-112). Here now the main question raised is how noisy, warm and wet brain parenchymal environment may support such mechanism. To answer these questions, some studies proposed the potential roles of Hameroff-Penrose microtubular π- electron Bose-Einstein condensation, Fröhlich condensation, and quantum electron neurosynaptic tunneling (109-112). In our integrative quantum-neuroholographic *QFT* model of consciousness where the classical neural, neuroquantum and quantum-gravitational aspects of consciousness are all treated on equal basis in their common, combined and integrated contribution to the consciousness phenomenon and qualia, the *SSB* plays the central role as so-called quantum neurodynamical consciousness medium in which mental neuroholographic representations and their mind dynamics takes place (100). In our opinion, it remains plausible that, phenomenologically speaking, neuroquantum processes take part in global, general consciousness neurodynamics. Consciousness may exhibit phenomenology consistent with quantum-like dynamics combined with the classical one (31, 50-53). Therefore, we may say that consciousness is a very complex, multiscale classical-quantum phenomenon occurring at mesoscopic, semiclassical scale acting as a bridge between the two, quantum scale on the one side and classical one on the other. However, the question is of what origin is this quantum behaviour. Is it classically determined neuroquantum phenomenon or quantum-based classical phenomenon? Here, there are three possibilities: (i) highly neurointegrative extroversion of neuroquantum ultralevel on the high neurosystem scale level without classical reduction, so-called macroscopization of neuroquantum phenomena in the brain (56, 63), (ii) supersystemic neuroquantum-like behaviour of complex classical brain system networks described by the laws of the theory of complex systems (113, 114), or (iii) both, i.e. the simultaneous co-existence of the two. But from the phenomenological point of view, in ether case, the quantum consciousness seems to operate and dominate in altered states of consciousness (50-53) while regular, normal states of consciousness are prominently characterized by classical brain neurodynamics (2, 10). Here, the question of qualia still remains elusive. In our opinion, besides Pribram's classical neuroholographic representations (62) and the Rudrauf-Bennequin's intrinsic projective perspective (115) of a neural system generating and autoperceiving them in a retrograde manner, which are essential for it, neuroquantum microscopic scale certainly plays some role in qualia toning that determines the strength of impression feeling of the qualia with maybe even quantum-gravitational involvement qualitatively speaking but quantitatively of course in a much lesser extent then it is in transpersonal and altered states of consciousness (50-53, 100).

Future Directions

Neuromethodologically speaking, the next steps in theoretical computational neuromodeling of consciousness as well as in neurologically-psychiatric clinical research include building (i) numerical simulations of training *CA-SOM* on naturalistic inputs, evaluating attractor neurodynamics, $I(H;S)$ trajectories, and neurooscillatory gating as well as comparison with behavioral switching and perceptual stability, (ii) experimental tests with lesion or temporarily inactivated neurotopographic hubs (e.g., with *TMS*), quantification effects on stable content formation, manipulation of gamma neurosynchrony and testing attractor dwell

times and neural binding (6, 41-44, 69), (iii) parameter inference and fitting *CA-SOM* to *ECoG/MEG/fMRI* datasets, validating cortical laminar/neurooscillatory predictions and workspace ignition signatures (68, 69), (iv) theoretical extensions of the model that would incorporate multi-attractor sequences (working memory), action selection coupling (basal ganglia neural loops), and neuromodulatory control (adaptive α_{eff} and σ), (v) subject-specific large-scale network models that integrate realistic structural connectivity (e.g., diffusion *MRI*-based connectomes), laminar-specific populations, and thalamic nodes, (vi) calibrating them to resting and task *fMRI/MEG/EEG* and (vii) testing the predicted shifts in ignition thresholds under controlled neuromodulatory and thalamic manipulations (15, 23, 25, 81, 106). Perturb-and-measure experiments (e.g., *TMS-EEG PCI*) can probe where the system sits relative to the ignition bifurcation and how it moves under arousal changes. Laminar *M/EEG* and intracranial recordings can test the predicted enhancement of alpha/beta-to-gamma cross-frequency neurocoupling during consciousness access (14, 22, 25). Finally, learning experiments can test whether conscious access indeed gates neurosynaptic consolidation via neuromodulated three-factor rules.

Conclusion

We have articulated a cortical theory of consciousness grounded in classical neurodynamics but capable of being derived as a classical limit from a deeper stochastic quantum field. Conscious access emerges when neurostructurally grounded, biophysically plausible cortical circuits achieve a metastable regime of global integration coordinated through thalamocortical synchrony and modulated by neuromodulators. The *CA-SOM* architecture explains how the neocortex's topography and neurorecurrence generate stable, integrated, and specific conscious contents. This regime is captured by a macroscopic order parameter $C(t)$, whose onset corresponds to an eigenvalue crossing in mean-field meurodynamics and whose maintenance involves retrograde neurofeedback on gains, neurocouplings, and neuroplasticity. The retrograde neurofeedback laws close the loop between content and substrate, aligning the theory with empirical phenomena in attention, predictive coding, and workspace ignition. The framework reconciles diverse empirical signatures across behavior, neuroelectrophysiology, and imaging, and it integrates physics by showing that any putative sub-neural quantum effects reduce to classical stochastic contributions at the scales relevant for cognition. It offers testable predictions for neuroscience and practical levers for neuromodulation and therapy. By uniting cortical neurocitoarchitecture, network neurodynamics, and physical constraints, the theory advances a principled and mechanistic understanding of how the brain generates and uses consciousness access. Even if future data never support quantum contributions at neurobiological scales, the classical *CA-SOM* provides a mechanistic, testable, and neurostructurally faithful account of how cortical neural circuits can generate conscious experience.

Acknowledgement

This work was supported by the Ministry of Science and Technological Development of the Republic of
Serbia.

References

1. Dehaene S. Consciousness and the Brain. New York: Viking. 2014.doi:

2. Dehaene S, Changeux JP. Experimental and theoretical approaches to conscious processing. Neuron. 2011;70(2):200-27.doi: 10.1016/j.neuron.2011.03.018
3. Lamme V, Roelfsema P. The distinct modes of vision offered by feedforward and recurrent processing. Trends Cogn Sci. 2000;4(6):301-9.doi:
4. Mashour GA, Roelfsema P, Changeux JP, Dehaene S. Conscious Processing and the Global Neuronal Workspace Hypothesis. Neuron. 2020;105(5):776-98.doi: 10.1016/j.neuron.2020.01.026
5. Oizumi M, Albantakis L, Tononi G. From the phenomenology to the mechanisms of consciousness: Integrated Information Theory 3.0. PLoS Comput Biol. 2014;10(5):e1003588.doi: 10.1371/journal.pcbi.1003588
6. Singer W. Neuronal synchrony: a versatile code for the definition of relations? Neuron. 1999;24(1):49-65, 111-25.doi: 10.1016/s0896-6273(00)80821-1
7. Varela F, Lachaux JP, Rodriguez E, Martinerie J. The brainweb: phase synchronization and large-scale integration. Nat Rev Neurosci. 2001;2(4):229-39.doi: 10.1038/35067550
8. Lamme VA. Towards a true neural stance on consciousness. Trends Cogn Sci. 2006;10(11):494-501.doi: 10.1016/j.tics.2006.09.001
9. Baars BA. Cognitive Theory of Consciousness. Cambridge University Press. 1988.doi:
10. Tononi G. An information integration theory of consciousness. BMC Neurosci. 2004;5:42.doi: 10.1186/1471-2202-5-42
11. Bastos AM, Usrey WM, Adams RA, Mangun GR, Fries P, Friston KJ. Canonical microcircuits for predictive coding. Neuron. 2012;76(4):695-711.doi: 10.1016/j.neuron.2012.10.038
12. Buzsáki G. Rhythms of the Brain. Oxford: Oxford University Press. 2006.doi:
13. Caldeira A, Leggett A. Path integral approach to quantum Brownian motion. Physica A. 1983;121(3):587-616.doi:
14. Canolty RT, Knight RT. The functional role of cross-frequency coupling. Trends Cogn Sci. 2010;14(11):506-15.doi: 10.1016/j.tics.2010.09.001
15. Deco G, Jirsa VK, McIntosh AR. Emerging concepts for the dynamical organization of resting-state activity in the brain. Nat Rev Neurosci. 2011;12(1):43-56.doi: 10.1038/nrn2961
16. Douglas RJ, Martin KA. Neuronal circuits of the neocortex. Annu Rev Neurosci. 2004;27:419-51.doi: 10.1146/annurev.neuro.27.070203.144152
17. Friston K. The free-energy principle: a unified brain theory? Nat Rev Neurosci. 2010;11(2):127-38.doi: 10.1038/nrn2787
18. Halassa MM, Kastner S. Thalamic functions in distributed cognitive control. Nat Neurosci. 2017;20(12):1669-79.doi: 10.1038/s41593-017-0020-1
19. Harris KD, Shepherd GM. The neocortical circuit: themes and variations. Nat Neurosci. 2015;18(2):170-81.doi: 10.1038/nn.3917
20. Larkum M. A cellular mechanism for cortical associations: an organizing principle for the cerebral cortex. Trends Neurosci. 2013;36(3):141-51.doi: 10.1016/j.tins.2012.11.006
21. Markram H, Muller E, Ramaswamy S, Reimann MW, Abdellah M, Sanchez CA, et al. Reconstruction and Simulation of Neocortical Microcircuitry. Cell. 2015;163(2):456-92.doi: 10.1016/j.cell.2015.09.029
22. Michalareas G, Vezoli J, van Pelt S, Schoffelen JM, Kennedy H, Fries P. Alpha-Beta and Gamma Rhythms Subserve Feedback and Feedforward Influences among Human Visual

Cortical Areas. Neuron. 2016;89(2):384-97.doi: 10.1016/j.neuron.2015.12.018
23. Saalmann YB, Pinsk MA, Wang L, Li X, Kastner S. The pulvinar regulates information transmission between cortical areas based on attention demands. Science. 2012;337(6095):753-6.doi: 10.1126/science.1223082
24. Aston-Jones G, Cohen JD. An integrative theory of locus coeruleus-norepinephrine function: adaptive gain and optimal performance. Annu Rev Neurosci. 2005;28:403-50.doi: 10.1146/annurev.neuro.28.061604.135709
25. Buzsáki G, Tingley D. Space and Time: The Hippocampus as a Sequence Generator. Trends Cogn Sci. 2018;22(10):853-69.doi: 10.1016/j.tics.2018.07.006
26. Frémaux N, Gerstner W. Neuromodulated Spike-Timing-Dependent Plasticity, and Theory of Three-Factor Learning Rules. Front Neural Circuits. 2015;9:85.doi: 10.3389/fncir.2015.00085
27. Lillicrap TP, Santoro A, Marris L, Akerman CJ, Hinton G. Backpropagation and the brain. Nat Rev Neurosci. 2020;21(6):335-46.doi: 10.1038/s41583-020-0277-3
28. Miller EK, Cohen JD. An integrative theory of prefrontal cortex function. Annu Rev Neurosci. 2001;24:167-202.doi: 10.1146/annurev.neuro.24.1.167
29. Sara SJ. The locus coeruleus and noradrenergic modulation of cognition. Nat Rev Neurosci. 2009;10(3):211-23.doi: 10.1038/nrn2573
30. Schultz W. Predictive reward signal of dopamine neurons. J Neurophysiol. 1998;80(1):1-27.doi: 10.1152/jn.1998.80.1.1
31. Tegmark M. The Importance of Quantum Decoherence in Brain Processes. Physical review E, Statistical physics, plasmas, fluids, and related interdisciplinary topics. 2000;61:4194-206.doi: 10.1103/PhysRevE.61.4194
32. Buxhoeveden DP, Casanova MF. The minicolumn hypothesis in neuroscience. Brain. 2002;125(Pt 5):935-51.doi: 10.1093/brain/awf110
33. Markov NT, Vezoli J, Chameau P, Falchier A, Quilodran R, Huissoud C, et al. Anatomy of hierarchy: feedforward and feedback pathways in macaque visual cortex. J Comp Neurol. 2014;522(1):225-59.doi: 10.1002/cne.23458
34. Mountcastle VB. The columnar organization of the neocortex. Brain. 1997;120 (Pt 4):701-22.doi: 10.1093/brain/120.4.701
35. Amit D. Modeling Brain Function: The World of Attractor Neural Networks. Cambridge University Press. 1989.doi:
36. Cottrell M, Fort JC, Pagès G. Theoretical aspects of the SOM algorithm. In Proceedings of the WSOM 97, workshop on self-organizing maps. Helsinki University of Technology. 1997;21:119-38.doi:
37. Demircigil M, Heusel J, Löwe M, Upgang S, Vermet F. On a Model of Associative Memory with Huge Storage Capacity. Journal of Statistical Physics. 2017;168:288–99.doi: 10.1007/s10955-017-1806-y
38. Hopfield JJ. Neural networks and physical systems with emergent collective computational abilities. Proc Natl Acad Sci U S A. 1982;79(8):2554-8.doi: 10.1073/pnas.79.8.2554
39. Kohonen T. Self-Organizing Maps Springer. 2001.doi:
40. Felleman DJ, Van Essen DC. Distributed hierarchical processing in the primate cerebral cortex. Cereb Cortex. 1991;1(1):1-47.doi: 10.1093/cercor/1.1.1-a
41. Bastos AM, Vezoli J, Fries P. Communication through coherence with inter-areal delays. Curr Opin Neurobiol. 2015;31:173-80.doi: 10.1016/j.conb.2014.11.001

42. Fries P. Rhythms for Cognition: Communication through Coherence. Neuron. 2015;88(1):220-35.doi: 10.1016/j.neuron.2015.09.034
43. Gaillard R, Dehaene S, Adam C, Clémenceau S, Hasboun D, Baulac M, et al. Converging intracranial markers of conscious access. PLoS Biol. 2009;7(3):e61.doi: 10.1371/journal.pbio.1000061
44. Wang XJ. Neurophysiological and computational principles of cortical rhythms in cognition. Physiol Rev. 2010;90(3):1195-268.doi: 10.1152/physrev.00035.2008
45. Deco G, Kringelbach ML, Jirsa VK, Ritter P. The dynamics of resting fluctuations in the brain: metastability and its dynamical cortical core. Sci Rep. 2017;7(1):3095.doi: 10.1038/s41598-017-03073-5
46. Del Cul A, Baillet S, Dehaene S. Brain dynamics underlying the nonlinear threshold for access to consciousness. PLoS Biol. 2007;5(10):e260.doi: 10.1371/journal.pbio.0050260
47. Schlosshauer M. Decoherence, the Measurement Problem, and Interpretations of Quantum Mechanics. Reviews of Modern Physics. 2004;76(4):1267-305.doi: 10.1103/RevModPhys.76.1267
48. Schlosshauer-Selbach M. Decoherence and the Quantum-To-Classical Transition. 2007.doi: 10.1007/978-3-540-35775-9
49. Raković D. Quantum-holographic framework for consciousness and acupuncture: Psychosomatic-cognitive implications. Med Data Rev. 2011;3(3):303-13.doi:
50. Raković D. Quantum-Holistic Framework of Transpersonal Psychosomatics: Complete Healing and Spiritual Integration. International Journal of Supervision in Psychotherapy. 2021;2021:55-69.doi: 10.47409/ijsp.2021.3.4
51. Raković D. Quantum-Informational Macrophenomena in Biomedicine & Holistic Psychosomatics: Quantum-Holographic Framework. Psychology and Behavioral Science International Journal. 2022;19.doi: 10.19080/PBSIJ.2022.19.556015
52. Raković D. QUANTUM-HOLOGRAPHIC BASES OF PSYCHOSOMATICS & SPIRITUALITY: CONTRIBUTION TO COMPARATIVE EXPLORATION OF SCIENCE & RELIGION. SCIREA Journal of Sociology. 2023.doi: 10.54647/sociology841115
53. Rakovic D. On Tesla-inspired Extended Quantum-Holographic Framework for Reprogramming Macro-Quantum Correlations of Individual and Collective Consciousness. Journal of Human Psychology. 2024;2:14-9.doi: 10.14302/issn.2644-1101.jhp-24-5247
54. Raković D, Dugić M, Yu Rn. Quantum-holographic and classical Hopfield-like associative nnets: Implications for modeling two cognitive modes of consciousness. Opticheskii Journal. 2005;72:13-8.doi:
55. Caldeira A, Leggett A. Quantum tunnelling in a dissipative system. Ann Phys. 1983;149(2):374–456.doi:
56. Freeman W, Vitiello G. Nonlinear brain dynamics and many-body field dynamics. Electromagn Biol Med. 2006;25(1):45–53.doi:
57. Gabor D. A new microscopic principle. Nature. 1948;161(4098):777.doi: 10.1038/161777a0
58. Goldstone J. Field theories with "superconductor" solutions. Nuovo Cimento. 1961;19:154–64.doi:
59. Hänggi P, Ingold G. Fundamental aspects of quantum Brownian motion. Chaos. 2005;15(2):026105.doi:
60. Jibu M, Yasue K. Quantum Brain Dynamics and Consciousness. John Benjamins 1995.doi:
61. Parisi G, Wu Y. Perturbation theory without gauge fixing. Sci Sin. 1981;24:483–96.doi:

62. Pribram K. Brain and Perception: Holonomy and Structure in Figural Processing. Lawrence Erlbaum. 1991.doi:
63. Umezawa H. Advanced Field Theory: Micro, Macro, and Thermal Physics. AIP. 1993.doi:
64. Vitiello G. Dissipation and memory capacity in the quantum brain model. International Journal of Modern Physics B. 1995;09:973.doi: 10.1142/S0217979295000380
65. Zurek W. Decoherence, einselection, and the quantum origins of the classical. Rev Mod Phys. 2003;75(3):715–75.doi:
66. Fisher M. Quantum Cognition: The possibility of processing with nuclear spins in the brain. Annals of Physics. 2015;362:593-602.doi: 10.1016/j.aop.2015.08.020
67. Reimers J, McKemmish L, McKenzie R, Mark A, Hush N. Weak, strong, and coherent regimes of Fr??hlich condensation and their applications to terahertz medicine and quantum consciousness. Proceedings of the National Academy of Sciences of the United States of America. 2009;106:4219-24.doi: 10.1073/pnas.0806273106
68. Buschman TJ, Miller EK. Top-down versus bottom-up control of attention in the prefrontal and posterior parietal cortices. Science. 2007;315(5820):1860-2.doi: 10.1126/science.1138071
69. Dehaene S, Charles L, King J-R, Marti S. Toward a computational theory of conscious processing. Current opinion in neurobiology. 2014;25C:76-84.doi: 10.1016/j.conb.2013.12.005
70. Friston K. A theory of cortical responses. Philos Trans R Soc Lond B Biol Sci. 2005;360 (1456):815–36.doi:
71. Kanai R, Komura Y, Shipp S, Friston K. Cerebral hierarchies: predictive processing, precision and the pulvinar. Philos Trans R Soc Lond B Biol Sci. 2015;370 (1668):20140169.doi:
72. Rao R, Ballard D. Predictive coding in the visual cortex: a functional interpretation. Nat Neurosci. 1999;2(1):79–87.doi:
73. Casali AG, Gosseries O, Rosanova M, Boly M, Sarasso S, Casali KR, et al. A theoretically based index of consciousness independent of sensory processing and behavior. Sci Transl Med. 2013;5(198):198ra05.doi: 10.1126/scitranslmed.3006294
74. Gardiner C. Handbook of Stochastic Methods. Springer. 1985.doi:
75. Gardiner C. Stochastic Methods: A Handbook for the Natural and Social Sciences. 4th ed. Berlin: Springer. 2009.doi:
76. Risken H. The Fokker–Planck Equation. Springer. 1984.doi:
77. Risken H. The Fokker-Planck Equation: Methods of Solution and Applications. 2nd ed. Berlin: Springer. 1996.doi:
78. Murphy PR, Robertson IH, Balsters JH, O'Connell R G. Pupillometry and P3 index the locus coeruleus-noradrenergic arousal function in humans. Psychophysiology. 2011;48(11):1532-43.doi: 10.1111/j.1469-8986.2011.01226.x
79. Wilson HR, Cowan JD. Excitatory and inhibitory interactions in localized populations of model neurons. Biophys J. 1972;12(1):1-24.doi: 10.1016/s0006-3495(72)86068-5
80. Buckley C, Kim CS, McGregor S, Seth A. The free energy principle for action and perception: A mathematical review2017.
81. Honey CJ, Sporns O, Cammoun L, Gigandet X, Thiran JP, Meuli R, et al. Predicting human resting-state functional connectivity from structural connectivity. Proc Natl Acad Sci U S A. 2009;106(6):2035-40.doi: 10.1073/pnas.0811168106
82. Attwell D, Laughlin SB. An energy budget for signaling in the grey matter of the brain. J Cereb Blood Flow Metab.

2001;21(10):1133-45.doi: 10.1097/00004647-200110000-00001
83. Joglekar MR, Mejias JF, Yang GR, Wang XJ. Inter-areal Balanced Amplification Enhances Signal Propagation in a Large-Scale Circuit Model of the Primate Cortex. Neuron. 2018;98(1):222-34.e8.doi: 10.1016/j.neuron.2018.02.031
84. Kuramoto Y. Chemical Oscillations, Waves, and Turbulence. Berlin: Springer. 1984.doi:
85. Canolty RT, Edwards E, Dalal SS, Soltani M, Nagarajan SS, Kirsch HE, et al. High gamma power is phase-locked to theta oscillations in human neocortex. Science. 2006;313(5793):1626-8.doi: 10.1126/science.1128115
86. Robbins H, Monro S. A stochastic approximation method. Ann Math Stat. 1951;22(3):400–7.doi:
87. Penfield W, Rasmussen T. The Cerebral Cortex of Man. Macmillan. 1950.doi:
88. Wandell BA, Dumoulin SO, Brewer AA. Visual field maps in human cortex. Neuron. 2007;56(2):366-83.doi: 10.1016/j.neuron.2007.10.012
89. Krotov D, Hopfield J. Dense Associative Memory Is Robust to Adversarial Inputs. Neural Comput. 2018;30(12):3151-67.doi: 10.1162/neco_a_01143
90. Ramsauer H, Schäfl B, Lehner J, Seidl P, Widrich M, Gruber L, et al. Hopfield Networks is All You Need2020.
91. Khalil H. Nonlinear Systems. 3rd ed. . Prentice Hall. 2002.doi:
92. Cover T, Thomas J. Elements of Information Theory. 2nd ed. . Wiley. 2006.doi:
93. Ford G, Kac M, Mazur P. Statistical mechanics of assemblies of coupled oscillators. J Math Phys. 1965;6(4):504–15.doi:
94. Peruš M, Loo CK. Holonomic Brain Processes. 2010.
95. Peruš M, Loo CK. Quantum Neural Information Processing. 2011. p. 217-21.
96. Peruš M, Loo CK. Derivation of Quantum Associative Network from Hopfield-Like ANN and HNeT. 2011. p. 199-216.
97. McFadden J. Conscious Electromagnetic (CEMI) Field Theory. NeuroQuantology. 2007;5.doi: 10.14704/nq.2007.5.3.135
98. Baars BJ, Franklin S. How conscious experience and working memory interact. Trends Cogn Sci. 2003;7(4):166-72.doi: 10.1016/s1364-6613(03)00056-1
99. Ramamurthy U, Baars B, K DM, Franklin S. LIDA: A working model of cognition. Proceedings of the 7th International Conference on Cognitive Modeling. 2006.doi:
100. Grbatinić I, Medarević A, Raković D. The Integrative Quantum-Neuroholographic Field Model of the Consciousness System. Neuroquantology. 2025;23(10):82-104.doi:
101. Hameroff S. Quantum computation in brain microtubules? The Penrose-Hameroff 'Orch OR' model of consciousness. Philosophical Transactions of The Royal Society B: Biological Sciences. 1998;356.doi: 10.1098/rsta.1998.0254
102. Hameroff S. Consciousness Is Quantum State Reduction Which Creates the Flow of Time. Timing & Time Perception. 2023;12:1-10.doi: 10.1163/22134468-bja10098
103. Hameroff S, Penrose R. Consciousness in the universe: a review of the 'Orch OR' theory. Phys Life Rev. 2014;11(1):39-78.doi: 10.1016/j.plrev.2013.08.002
104. Logothetis NK, Pauls J, Augath M, Trinath T, Oeltermann A. Neurophysiological investigation of the basis of the fMRI signal. Nature. 2001;412(6843):150-7.doi: 10.1038/35084005
105. McFadden J. Integrating information in the brain's EM field: the cemi field theory of consciousness. Neurosci Conscious. 2020;2020(1):niaa016.doi: 10.1093/nc/niaa016

106. Shine JM, Hearne LJ, Breakspear M, Hwang K, Müller EJ, Sporns O, et al. The Low-Dimensional Neural Architecture of Cognitive Complexity Is Related to Activity in Medial Thalamic Nuclei. Neuron. 2019;104(5):849-55.e3.doi: 10.1016/j.neuron.2019.09.002
107. He BJ. Scale-free brain activity: past, present, and future. Trends Cogn Sci. 2014;18(9):480-7.doi: 10.1016/j.tics.2014.04.003
108. Murray JD, Bernacchia A, Freedman DJ, Romo R, Wallis JD, Cai X, et al. A hierarchy of intrinsic timescales across primate cortex. Nat Neurosci. 2014;17(12):1661-3.doi: 10.1038/nn.3862
109. Marshall IN. Consciousness and Bose-Einstein condensates. New Ideas in Psychology. 1989 7(1):73–83.doi:
110. Vitiello M. Quantum Dissipation and Information: A route to consciousness modeling. NeuroQuantology. 2003;2:266-79.doi:
111. Walker EH.
The Physics of Consciousness: The Quantum Mi nd and the Meaning of Life. Perseus Books. 2000.doi:
112. Zohar D.
The Quantum Self: Human Nature and Consciou sness Defined by the New Physics William Morr ow and Company, Inc. 1990.doi:
113. Khrennikov A. Ubiquitous Quantum Structure: From Psychology to Finance. Springer Science & Business Media. 2010.doi:
114. Tognoli E, Kelso JAS. The metastable brain. Neuron. 2014;81:35–48.doi:
115. Rudrauf D, Bennequin D, Granic I, Landini G, Friston K, Williford K. A mathematical model of embodied consciousness. J Theor Biol. 2017;428:106-31.doi: